Atmos. Chem. Phys. Discuss., https://doi.org/10.5194/acp-2018-1158
Manuscript under review for journal Atmos. Chem. Phys.
Discussion started: 6 May 2019

Atmospheric Chemistry and Physics Discussions

Evaluation and uncertainty investigation of the NO_2, CO and NH_3 modeling over China under the framework of MICS-Asia III

Lei Kong[1,3], Xiao Tang[2,3], Jiang Zhu[1,3], Zifa Wang[2,3], Joshua S. Fu[4], Xuemei Wang[5], Syuichi Itahashi[6,7], Kazuyo Yamaji[8], Tatsuya Nagashima[9], Hyo-Jung Lee[10], Cheol-Hee Kim[10], Chuan-Yao Lin[11], Lei Chen[2,3], Meigen Zhang[2,3], Zhining Tao[12,13], Jie Li[2,3], Mizuo Kajino[14,15], Hong Liao[16], Kengo Sudo[17], Yuesi Wang[2,3], Yuepeng Pan[2,3], Guiqian Tang[2,3], Meng Li[18,19], Qizhong Wu[20,21]; Baozhu Ge[2,3], Gregory R. Carmichael[22]

[1]ICCES, Institute of Atmospheric Physics, Chinese Academy of Sciences, Beijing, 100029, China
[2]LAPC, Institute of Atmospheric Physics, Chinese Academy of Sciences, Beijing, 100029, China
[3]University of Chinese Academy of Sciences, Beijing, 100049, China
[4]Department of Civil and Environmental Engineering, University of Tennessee, Knoxville, TN, 37996, USA
[5]Institite for Environment and Climate Research, Jinan University, Guangzhou, 510632, China
[6]Central Research Institute of Electric Power Industry, Abiko, Chiba, 270-1194, Japan
[7]Department of Marine, Earth, and Atmospheric Sciences, North Carolina State University, Raleigh, NC 27607, USA
[8]Graduate School of Maritime Sciences, Kobe University, Kobe, Hyogo 658-0022, Japan
[9]National Institute for Environmental Studies, Onogawa, Tsukuba 305-8506, Japan
[10]Department of Atmospheric Sciences, Pusan National University, Busan, 46241, South Korea
[11]Research Center for Environmental Changes, Academia Sinica, Taipei, 115, Taiwan
[12]Universities Space Research Association, Columbia, MD, USA
[13]NASA Goddard Space Flight Center, Greenbelt, MD, 130, USA
[14]Meteorological Research Institute, Japan Meteorological Agency, Tsukuba, Ibaraki, 305-0052, Japan
[15]Faculty of Life and Environmental Sciences, University of Tsukuba, Tsukuba, Ibaraki, 305-8577, Japan
[16]School of Environmental Science and Engineering, Nanjing University of Information Science & Technology, Nanjing 210044, China
[17]Graduate School of Environmental Studies, Nagoya University, Nagoya, Japan
[18]Ministry of Education Key laboratory for Earth System Modeling, Department of Earth System Science, Tsinghua University, Beijing, 100084, China
[19]Multiphase Chemistry Department, Max Planck Institute for Chemistry, Mainz, 55128, Germany
[20]College of Global Change and Earth System Science, Beijing Normal University, Beijing 100875, China
[21]Joint Centre for Global Changes Studies, Beijing Normal University, Beijing 100875, China
[22]Center for Global and Regional Environmental Research, University of Iowa, Iowa City, IA, 52242, USA

Correspondence to: Xiao Tang(tangxiao@mail.iap.ac.cn)

Abstract. Despite significant progress in improving chemical transport models (CTMs), applications of these modeling endeavours are still subject to the large and complex model uncertainty. Model Inter-Comparison Study for Asia III (MICS-Asia III) provides the opportunity to assess the capability and uncertainty of current CTMs in East Asia applications. In this study, we evaluated the multi-model simulations of nitrogen dioxide (NO_2), carbon monoxide (CO) and ammonia (NH_3) over China under the framework of MICS-Asia III. Compared with MICS-Asia II, modeling results were provided by a larger number of independent groups from different countries/regions and covered a longer period of time (one-full year). Furthermore, most of these groups used a common emission inventory, common meteorological inputs, and the same modeling domain and horizontal resolutions. New observations over North China Plain (NCP) and Peral River Delta (PRD) were also

Atmos. Chem. Phys. Discuss., https://doi.org/10.5194/acp-2018-1158
Manuscript under review for journal Atmos. Chem. Phys.
Discussion started: 6 May 2019

Atmospheric Chemistry and Physics Discussions

available in MICS-Asia III, allowing model evaluations over highly industrialized regions. The results show that most models well captured the monthly and spatial patterns of NO_2 in NCP though NO_2 levels were slightly underestimated. Relatively poor performance in NO_2 simulations was found in PRD with larger root mean square error and lower spatial correlation coefficients, possibly due to the relative coarse model resolutions. All models significantly underpredicted CO concentrations both in NCP and PRD, with annual mean concentrations 65.4% and 61.4% underestimated by the ensemble mean respectively. Such large underestimations suggest that CO emissions might be underestimated in current emission inventory. In contrast to the good skills in simulating the monthly variations of NO_2 and CO concentrations, all models failed to reproduce the observed monthly variations of NH_3 concentrations in NCP. Most models mismatched the observed peak in July and showed negative correlation coefficients with observations, which may be closely related to the uncertainty in the monthly variations of NH_3 emissions and the NH_3 gas-aerosol partitioning. Finally, inter-comparisons of these model results were conducted to quantify the impacts of model uncertainty on the simulations of these gases, which are shown increase with the reactivity of species. Models contained more uncertainty in the NH_3 simulations. This suggests that for some highly active and/or short-lived primary pollutants, like NH_3, model uncertainty can also take a great part in the forecast uncertainty in addition to the emission uncertainty. Based on these results, some recommendations are made for future studies.

1 Introduction

As the rapid growth in East Asia's economy with surging energy consumption and emissions, air pollution has become an increasingly important scientific topic and political concern in East Asia due to its significant environmental and health effects (Lelieveld et al., 2015). Chemical transport models (CTMs), serving as a critical tool both in scientific research and policy makings, have been applied into various air quality issues, including air quality prediction, long-range transport of atmospheric pollutants, development of emission control strategies and understanding of observed chemical phenomena. However, challenges still remain in the air quality modeling due to the multi-scale and non-linear nature of the complex atmospheric processes (Carmichael et al., 2008). Air quality modeling still suffers from large uncertainties related to missing or poorly parameterized physical and chemical processes, inaccurate and/or incomplete emission inventories as well as poorly represented initial and boundary conditions (Carmichael et al., 2008). Understanding such uncertainties and their impacts on air quality modeling is of great importance in assessing the robustness of models for their applications in scientific research and operational use.

There are specific techniques to assess these uncertainties. Monte Carlo simulations, based on different values of model parameters or input fields sampled from a predefined probability density function (PDF), can provide an approximation to the PDF of possible model output and serves as an excellent characterization of the uncertainties of simulations (Hanna et al., 2001). However, this method is more suited to deal with the uncertainty related to the continuous variables, such as input data or parameters in parameterization. The ensemble method, based on a set of different models, is an alternative approach to accounting for the range of uncertainties (Galmarini et al., 2004;Mallet and Sportisse, 2006). In Europe and North America,

the Air Quality Model Evaluation International Initiative (AQMEII) has been implemented to investigate the model uncertainties of their regional-scale model predictions (Rao et al., 2011). The Model Inter-Comparison Study for Asia (MICS-Asia) provides the opportunity to assess the model performances and uncertainties in East Asia applications. The first Phase of MICS-Asia (MICS-Asia I) was initiated in 1998 and carried out during period 1998–2002, mainly focusing on the long-range transport and depositions of sulfur in Asia (Carmichael et al., 2002). In 2003, the second phase (MICS-Asia II) was initiated and took account of more species related to the regional health and ecosystem protection, including nitrogen compounds, O_3 and aerosols. Launched in 2010, MICS-Asia III greatly expanded the study scope by covering three individual and interrelated topics: (1) evaluate strength and weaknesses of current multi-scale air quality models and provide techniques to reduce uncertainty in Asia; (2) develop a reliable anthropogenic emission inventories in Asia and understanding uncertainty of bottom-up emission inventories in Asia; (3) provide multi-model estimates of radiative forcing and sensitivity analysis of short-lived climate pollutants.

This study addresses one component of topic 1, mainly focusing on the three gas pollutants of NO_2, CO and NH_3. Compared with MICS-Asia II, more modeling results (fourteen different models with thirteen regional models and one global model) were brought together within the topic 1 of MICS-Asia III, each run by independent modeling groups in China, Japan, Korea, United States of America and other countries/regions. The different models contain differences in their numerical approximations (mesh size, time step, chemical solver, etc.) and parameterizations, which represent a sampling of uncertainties residing in the air quality modeling. It would be difficult to interpret the results from intercomparison studies when the models are operated using different meteorological fields and emission inventories. Thus, in MICS-Asia III the models were constrained to be operated under the same conditions by using a common emission inventory, meteorological fields, modeling domain and horizontal resolutions. The simulations were also extended from the four months in MICS-Asia II to one-full year of 2010.

NO_2, CO and NH_3 are three important primary gas pollutants that has wide impacts on the atmospheric chemistry. As a major precursor of O_3, NO_2 plays an important role in the tropospheric O_3 chemistry, and can also lead to rainwater acidification and secondary aerosol formations by forming nitric acid (HNO_3) through oxidations (Dentener and Crutzen, 1993;Evans and Jacob, 2005). CO is a colorless and toxic gas ubiquitous throughout the atmosphere which is of interest as an indirect greenhouse gas (Gillenwater, 2008) and a precursor for tropospheric O_3 (Steinfeld, 1998). Being the major sink of OH, CO also controls the atmosphere's oxidizing capacity (Levy, 1971; Novelli et al., 1998). As the only primary alkaline gas in the atmosphere, NH_3 is closely associated with the acidity of precipitations for one thing, for another it could react with sulfuric acid and nitric acid forming ammonium sulfate and ammonium nitrate which account for a large proportion of the inorganic constituents of the fine particulate matter (Sun et al., 2012;Sun et al., 2013). Assessing their model performances is thus important to help us better understand their environmental consequences and also help explain the model performances for their related secondary air pollutants, such as O_3 and fine particulate matter.

In previous phase of MICS-Asia, no specific evaluation and inter-comparison work has been conducted for these gases, especially for CO and NH_3. In MICS-Asia II, model performance of NO_2 was evaluated as a relevant species to O_3(Han, Z. et

al., 2008), however such evaluations were limited to the observation sites from EANET (Acid Deposition Monitoring Network in East Asia). Model evaluations and inter-comparisons in industrialized regions of China has not been performed due to the limited number of monitoring sites in China from EANET, which hindered our understanding of the model performance in industrialized regions. More densely observations over highly industrialized regions of China, namely North China (NCP) and Peral River Delta (PRD), were first included in MICS-Asia III, allowing the model evaluations over highly industrialized regions. Meanwhile, emission inventories of these three gases are still subject to large uncertainties (Kurokawa et al., 2013;Li et al., 2017), which is a major source of uncertainties in air quality modeling and forecast. Evaluating these gases' emission inventories from a model perspective is a useful way to identify the uncertainties in emission inventory (Han, K. M. et al., 2008;Noije et al., 2006;Stein et al., 2014;Uno et al., 2007).

This study is aimed at the evaluation of the NO_2, CO and NH_3 simulations using the multi-model data from MICS-Asia III. Three questions are addressed: (1) what is the performance of current CTMs in simulating NO_2, CO and NH_3 over highly industrialized regions of China; (2) what are the potential factors responsible for the model deviations from observations and differences among models; and (3) how large are the model uncertainties on the simulations of these gases.

2 Intercomparison frameworks

2.1 Description on participating models and input data

Table 1 summarizes the chemical transport models participating in the MICS-Asia III as well as their configurations. These models included NAQPMS (Wang et al., 2001), two version of CMAQ (Byun and Schere, 2006), WRF-Chem (Grell et al., 2005), NU-WRF (Tao et al., 2013; Peters-Lidard et al., 2015), NHM-Chem (Kajino et al., 2018) and GEOS-Chem (http://acmg.seas.harvard.edu/geos/). All models employed the same modeling domain (Fig. 1) and horizontal resolutions (45km×45km) except M13 (0.5° of latitude×0.667° of longitude) and M14 (64km×64km).

Standard model input datasets of raw meteorological fields, emission inventory and boundary conditions were provided by MICS-Asia III for all participants. Raw meteorological fields were generated from a whole year simulations of 2010 using Weather Research and Forecasting Model (WRF) version 3.4.1 (Skamarock, 2008) with 45km×45km horizontal resolution in a lambert conform projection and vertically 40 layers from surface to the model top (10hPa). Initial and lateral boundary conditions (IC & BC) for meteorological simulation were generated every six hours using 1°×1° NCEP FNL (Final) Operational Global Analysis data (ds083.2). Real-time, global, sea surface temperature (RTG_SST_HR) analysis were used to generate and update lower BC for sea areas. Four-dimensional data assimilation nudging (Gridded FDDA & SFDDA) was performed during the simulation to increase the accuracy of WRF after the Objective Analysis with NCEP FNL (Final) Operational Global Analysis data (ds083.2), NCEP ADP Global Surface Observation Weather Data (ds461.0) and NCEP ADP Global Upper Air and Surface Weather Data (ds337.0).

Standard emission inventory provided by MICS-Asia III were used by all participants. The anthropogenic emissions were provided by a newly developed anthropogenic emission inventory for Asia (MIX) which integrated five national or regional

inventories, including REAS (Regional Emission inventory in Asia) inventory for Asia developed at the Japan National Institute for Environment Studies (NIES), the Multi-resolution Emission Inventory for China (MEIC) developed at Tsinghua University, the high-resolution ammonia emission inventory in China developed at Peking University, the Indian emission inventory developed at Argonne National Laboratory in the United States and the CAPSS (Clean Air Policy Support System) Korean emission inventory developed at Konkuk University (Li et al., 2017). Hourly biogenic emissions for the entire year of 2010 in MICS-Asia III were provided by the Model of Emissions of Gases and Aerosols from Nature version 2.04 (MEGANv2.04; Guenther et al., 2006). The Global Fire Emissions Database 3 (GFEDv3; Randerson et al., 2013) was employed for biomass burning emissions. Volcanic SO_2 emissions were provided by the Asia Center for Air Pollution Research (ACAP) with a daily temporal resolution. Air and ship emissions with an annual resolution were provided by the HTAPv2 emission inventory for 2010 (Janssens-Maenhout et al., 2015). NMVOC emissions were spectated into the model-ready inputs for three chemical mechanisms: CBMZ, CB05 and SAPRC-99 and the weekly and diurnal profiles for emissions were also provided.

MICS-Asia III provides two sets of top and lateral boundary conditions of the modeling domain for the year 2010, which were derived from the 3-hourly global CTM outputs of CHASER (Sudo et al., 2002a; Sudo et at., 2002b) and GEOS-Chem (http://acmg.seas.harvard.edu/geos/) run by Nagoya University (Japan) and the University of Tennessee (USA), respectively. GEOS-Chem was run with 2.5º×2º resolution and 47 vertical layers while CHASER model was run with 2.8º×2.8º and 32 vertical layers.

All participants were required to use the standard model input data to drive their model run so that impacts of model input data on simulations could be minimized. However, models are quite different from each other, and it is difficult to keep all the inputs the same. The majority of models have applied the standard meteorology fields, while some other models utilized their own meteorology models, including GEOS-Chem and RAMS-CMAQ. GEOS-Chem was driven by the GEOS-5 assimilated meteorological fields from the Goddard Earth Observing System of the NASA Global Modeling Assimilation Office, and The RAMS-CMAQ was driven by meteorological fields provided by Regional Atmospheric Modeling System (RAMS; Pielke et al., 1992). WRF-Chem utilized the same meteorology model (WRF) as the standard meteorological simulation, but two of them considered the two-way coupling effects of pollutants and meteorological fields. The CTM part of NHM-Chem is coupled with the JMA's non-hydrostatic meteorological model (NHM; Saito et al., 2006), but an interface to convert a meteorological model output of WRF to a CTM input was implemented (Kajino et al., 2018). Thus, the standard meteorology field was used in the NHM-Chem simulation, too.

2.2 Data and statistical methods

All modeling groups performed a base year simulations of 2010 and were required to submit their modeling results according to the data protocol designed in MICS-Asia III. Gridded monthly concentrations of NO_2, CO, NH_3 and ammonium in the surface layer were used in this study. Note that modeling results from M3 and NH_3 simulations from M8 were excluded due to their incredible results, therefore only thirteen modeling results were actually used in this study.

Hourly observed concentrations of NO_2 and CO were collected over the NCP (19 stations) and PRD (13 stations) from the air quality network over North China (Tang et al., 2012) and the Pearl River Delta regional air quality monitoring network (PRD RAQMN), respectively. The air quality monitoring network over North China was set up by the Chinese Ecosystem Research Network (CERN), the Institute of Atmospheric Physics (IAP) and the Chinese Academy of Sciences (CAS) since 2009 within an area of 500×500 km^2 in northern China. All monitoring stations were selected and set up according to the US EPA method designations (Ji et al., 2012). The PRD RAQMN network was jointly established by the government of the Guangdong Province and the Hong Kong Special Administrative Region, consisting of 16 automatic air quality monitoring stations across the PRD (Zhong et al., 2013). Thirteen of these stations are operated by the Environmental Monitoring Centers in the Guangdong Province (this study used) while the other three located in Hong Kong (not included in this study) are managed by the Hong Kong Environmental Protection Department. Monthly averaged observations were then calculated for comparison with the simulated monthly surface NO_2 and CO concentrations.

NH_3 observations for long-term period are indeed challenging and limited due to its strong temporal and spatial variability, quick conversion of NH_3 from one phase to another and also its stickiness to the observational instruments (von Bobrutzki et al., 2010). Measurements of surface NH_3 concentrations in year 2010 were not available in this study, however, one-year measurement of monthly NH_3 concentrations over China was conducted by the Ammonia Monitoring Network in China (AMoN-China) during September of 2015 to August of 2016 (Pan et al., 2018), which was used as a reference dataset in this study. The AMoN-China was established based on the CERN and the Regional Atmospheric Deposition Observation Network in North China Plain (READ-NCP; Pan et al., 2012), consisting of 53 sites over the whole China with monthly integrated measurements using the passive diffusive technique. 11 stations located in the NCP were used in this study. Distributions of the observation stations of NO_2, CO and NH_3 over NCP and PRD as well as their total emissions in year 2010 provided by MICS-Asia III are presented in Fig. 1.

Mean bias error (MBE), normalized mean bias (NMB), root mean square error (RMSE) and correlation coefficient (R) were calculated for the assessment of model performances. Standard deviation of ensemble models was calculated to measure the ensemble spread and the impacts of model uncertainty. Coefficient of variation (hereinafter, CV), defined as the standard deviation divided by average with larger value denoting lower consistency among models, was also used to measure the impacts of model uncertainty in relative sense. However, by this definition, there is a tendency that lower concentrations are more likely associated with higher value of CV, thus we did not calculate the values of CV over model grids whose simulated concentrations were lower than 0.1 ppbv for NO_2 and NH_3, and 0.1 ppmv for CO respectively. March–May, Jun–August, September–November and December–February were used to define the season spring, summer, autumn and winter, respectively.

Atmos. Chem. Phys. Discuss., https://doi.org/10.5194/acp-2018-1158
Manuscript under review for journal Atmos. Chem. Phys.
Discussion started: 6 May 2019

3 Results

3.1 Evaluating the ensemble models with observations

To facilitate comparisons, the modeling results were interpolated to the observation stations by taking the value from the grid cell where the monitoring stations located. Model evaluation metrics defined in Sect. 2.2 were then calculated to evaluate the modeling results against the observations.

3.1.1 NO_2

Figure 2 displays the comparisons between the observed and simulated annual mean NO_2 concentrations sampled from different observation sites over NCP (2a) and PRD(2b) with calculated model evaluation metrics summarized in Table 2. M13 is not included in the evaluation of NO_2 since it submitted NO_x rather than NO_2. In general, the majority of models underpredicted NO_2 levels both in NCP and PRD. Calculated MBE (NMB) ranges from -6.54 ppbv (-28.4%) to -2.45 (-10.6%) ppbv over NCP and from -9.84 ppbv (-44.0%) to -1.84 ppbv (-8.2%) over PRD among the negatively-biased models. These underpredicted NO_2 concentrations may help explain the overpredicted O_3 concentrations by these models found in the companion MICS paper by Li, J. et al., 2019. O_3 productions can either increase with NO_x under NO_x limited conditions or decrease under the NO_x saturated (also called volatile organic compounds (VOCs) limited) conditions (Sillman, 1999). Both NCP and PRD are industrialized regions in China with high NO_x emissions (Fig. 1). Observations also showed that NCP and PRD are falling into or changing into the NO_x saturated regimes (Shao et al., 2009;Jin and Holloway, 2015). Therefore, the underestimated NO_2 concentrations may contribute to the overprediction in O_3 concentrations over these two regions and more details about the O_3 predictions can be found in the companion paper by Li, J. et al., 2019. M5, M8, M9 and M11 in NCP and M5, M8 and M11 in PRD were exceptions that overpredicted NO_2 concentrations. M11 showed good performances in predicting NO_2 levels in NCP with smallest RMSE, while M9 significantly overestimated NO_2 with largest MBE and RMSE. Simulated NO_2 by M8 in PRD was close to the observations with smallest RMSE. Meanwhile, we also found that models exhibited better NO_2 modeling skills in NCP than that in PRD with smaller bias and RMSE.

According to the spatial correlation coefficients (Table 2), all models well reproduced the main features of the spatial variability of NO_2 concentrations in NCP with correlation coefficients ranging from 0.57 to 0.70. However, models failed in capturing the spatial variability in PRD with correlation coefficients only ranged from 0.00 to 0.38. Such low correlation might be partly attributed to the coarser model resolution (45km) than that of the observations. Some local impacts on the NO_2 concentrations may not be well resolved by the model with 45km horizontal resolution, indicating models' weaknesses in representing the sub-grid processes.

Figure 3 presents the monthly timeseries of the observed and simulated regional mean NO_2 concentrations over NCP (3a) and PRD (3b) from January to December in 2010. The models well captured the monthly variations of NO_2 concentrations both in NCP and PRD. According to Table 2, the correlation coefficient ranges from 0.28 to 0.96 in NCP and from 0.52 to 0.95 in PRD. M8 showed the largest overestimation among all models in summer that MBE (NMB) can reach as 12.1 ppbv

(75.8%), which may help explain the low correlation of this model. M9 exhibited a significant overestimation in winter in NCP with MBE (NMB) up to 22.0 ppbv (79.3%) while much less overestimation or even underestimation (summer) in other seasons. This discrepancy may be explained by that M9 was an online coupled model considering the two-way coupling effects between meteorology and chemistry. During the period with heavy haze, the radiation can be largely reduced by aerosol dimming effects, leading to weakened photochemistry, lowered boundary layer height and the increase of NO_2 concentrations. Severe haze was reported to occur in North China in January 2010, with maximum hourly $PM_{2.5}$ concentration even reached as high as ~500 $\mu g/m^3$ in urban Beijing (Gao et al., 2018). Such high aerosol loadings in atmosphere could trigger interactions between chemistry and meteorology. Interestingly, M9 did not overestimate NO_2 during winter in PRD as in NCP. This might be related to the lower aerosol concentrations and weaker chemistry-and-meteorology coupling effects in PRD.

3.1.2 CO

Similar analyses were performed for CO modeling. All models significantly underestimated the annual mean CO concentrations both in NCP and PRD (Figs. 2c-d and Table 2). Calculated MBE (NMB) ranges from -1.69 ppmv (-76.2%) to -1.16 ppmv (-52.0%) in NCP and from -0.67 ppmv (-69.6%) to -0.50 ppmv (-52.3%) in PRD (Table 2). Such large biases in all the models are probably related to the bias in the CO emission inventory over China. Tang et al., 2013 estimated the CO emissions over Beijing and surrounding areas in the summer of 2010 using the ensemble Kalman filter and reported a significant underestimation in the *a priori* estimate of CO emissions. Over the latest decades, global models also reported CO underestimations in north hemisphere (Stein et al., 2014) and a number of global model inversion studies have been conducted to derive the optimized CO emissions, of which most studies reported a significant underestimation of CO emissions in their *a priori* estimates(Bergamaschi et al., 2000;Miyazaki et al., 2012;Petron et al., 2002;Petron et al., 2004). Our findings agree with these studies and indicate that more accurate CO emissions are needed in future studies. Model performance in simulating spatial variability of CO concentrations was still poor in PRD according to Table 2 that most models showed negative correlation coefficients.

Timeseries of the observed and simulated regional mean CO concentrations in NCP and PRD (Fig.3c-d) show that the models well reproduced the monthly variation of CO concentrations in NCP and PRD with high temporal correlation coefficients, except M5 in NCP (Table 2). All models, however, underestimated CO concentrations throughout the whole year and showed largest underestimations in winter that MBE (NMB) by ensemble mean can be up -2.1 ppmv (-64.9%) in NCP and -0.75 ppmv (-60.6%) in PRD.

3.1.3 NH_3

Figure 2e show the observed and simulated annual mean NH_3 concentrations over different sites in NCP. The NH_3 observations in 2010 were not available and the observed monthly mean NH_3 concentrations in NCP from September 2015 to August 2016 were used as a reference data in this study. Negative biases are expected according to the increasing trend of atmospheric ammonia during period 2003–2016 detected by recently retrievals from the Atmospheric Infrared Sounder (AIRS)

aboard NASA's Aqua satellite (Warner et al., 2016;Warner et al., 2017). Due to the interannual uncertainty, we mainly focused on the disparities among different models rather than the deviation from observations.

Large differences can be seen in simulated NH_3 concentrations from different models. M14 simulated very low concentrations and exhibited the largest negative biases with MBE (NMB) -12.2 ppbv (-66.3%). This may be related to the higher conversion rate of NH_3 to NH_4^+ in M14 which will be discussed in later part of this section. On the contrary, M9 provided much higher NH_3 concentrations with MBE (NMB) up to 21.8 ppbv (118.7%). For the CMAQ models, M1 and M2 exhibited higher NH_3 concentrations and larger spatial variability compared to other CMAQ models. Such discrepancy could be explained by that M1 and M2 are two model runs using CMAQ v5.0.2. The bi-directional exchange of NH_3 has been integrated into CMAQ from version 5.0. This module can simulate the emitted and deposited processes of NH_3 between atmosphere and the surfaces, allowing the additional NH_3 emissions to the atmosphere (US EPA Office of Research and Development).

As can be seen in Table 2, the observed spatial variations of NH_3 over NCP can be well reproduced by all models (R = 0.57-0.71), indicating that the spatial variations of current NH_3 emissions over NCP are reasonable. However, all models failed to capture the observed monthly variations of NH_3 concentrations with most models mismatching the observed NH_3 peak (July) and showing negative correlation coefficients except the M10 and M13 showing good temporal correlations of 0.64 and 0.65, respectively (Fig. 3e and Table 2). This is quite different from the model behavior in simulating the monthly variation of NO_2 and CO concentrations. As can be seen in Fig. 3e, the observation showed the peak concentrations of NH_3 in summer months and low concentrations in autumn and winter, which is consistent with the previous NH_3 observations in NCP (Shen et al., 2011;Xu et al., 2016;Meng et al., 2011). Newly derived satellite-measured NH_3 at 918 hPa averaged between September 2002 and August 2015 also demonstrated higher concentrations in spring and summer and lower concentrations in autumn and winter (Warner et al., 2016). However, all models predicted a peak concentration in November except M10 in August in and M13 in June.

Figure 4 presents the timeseries of NH_3 emission rates in NCP from January to December in 2010. The monthly variations of NH_3 concentrations simulated by most models were closely related to the variations of the NH_3 emissions. The simulated NH_3 concentrations had three peaks in June, August and November but exhibited a significant decrease in July, which was corresponding to the peaks and the drop of the NH_3 emission rates in these months. The strong relationship between the simulated NH_3 concentrations and emission rates suggests that the poor performance in reproducing the observed monthly variations of NH_3 concentrations is probably related to the uncertainties in the estimated monthly variations of NH_3 emissions by current emission inventories. This is consistent with the recent reconciled bottom-up and top-down estimates of agriculture ammonia emission in China by Zhang et al., 2018.

It is worth noting that the NH_3 simulations suggest that there are important uncertainties in the models beyond those due to emission uncertainty. In order to investigate this issue, the impact of the modeling of the NH_3 gas-aerosol partitioning on the NH_3 simulation was analyzed. Figure 5 displays the timeseries of the simulated total ammonium ($NH_x = NH_3 + NH_4^+$) concentrations in atmosphere along with the ratio of gaseous NH_3 to the total ammonium. Large discrepancy can be seen in

the simulated gas-aerosol partitioning of NH_3 from different models. Among the models, M7 and M9 had higher NH_3/NH_x ratio than other models, which means that the two models tended to retain more emitted NH_3 in gas phase and had higher NH_3 concentrations than other models. For example, M7 predicted comparable magnitude of total ammonium with most models, while gas NH_3 concentration in M7 accounted for more than 60% of total ammonium in summer and even 90% in winter and therefore was higher than most models. On the contrary, M14 showed a much lower NH_3/NH_x ratio and produced much lower NH_3 concentrations than most models. Moreover, most models showed lower NH_3/NH_x ratio in summer than other seasons, suggesting higher conversion rates of NH_3 from gas phase to aerosol phase in summer. This would be related to the higher yield of ammonium sulfate due to the enhanced photochemical oxidation activity in summer (Husain and Dutkiewicz, 1990) estimated by most models. However, different from the above model results, the NH_3 and NH_4^+observations over NCP by Shen et al., 2011;Xu et al., 2016 showed a lower NH_3/NH_x ratio and higher ammonium in autumn and wither. Although observed NH_4^+ was largest in summer at a rural site in Beijing, observed NH_3/NH_x ratio was still highest in summer by Meng et al., 2011. These results indicate that large uncertainties exist in modeling the seasonal variations of gaseous NH_3 and aerosol NH_4^+ partitioning. The formations of NH_4^+ mainly depends on the acid gas concentrations, temperature, water availability (Khoder, 2002) and the flux rates of NH_3 (Nemitz et al., 2001). Compared with spring and summer, the lower temperature and higher SO_2 and NO_x emissions should favor the gas-to-particle phase conversion and lead to higher NH_4^+ aerosol concentrations. This indicate that some reaction pathways of acid productions (H_2SO_4 or HNO_3) may be missed in current models, such as aqueous-phase and heterogeneous chemistry (Cheng et al., 2016;Wang et al., 2016;Zheng et al., 2015). Such uncertainty may be another important factor contributing to the misrepresented monthly variation of NH_3 concentrations in NCP by the models.

3.2 Quantifying the impacts of model uncertainty

In this section, we further investigate the differences between the ensemble models to quantify the impacts of model uncertainty on these gases' simulations. As we mentioned in Sect. 2, most of these models employed the same raw meteorology fields and emission inventories over China under the same modeling domain and horizontal resolutions, which composed an appropriate set for investigation of the model uncertainties.

Figures 6-8 present the simulated annual mean concentrations of NO_2, CO and NH_3 from thirteen modeling results. Spatial distributions of the simulated NO_2, CO and NH_3 from different models agreed well with each other, similar to the spatial distributions of their emissions as shown in Fig. 1. High NO_2 concentrations were mainly located in the north and central-east China and several hot-spots of NO_2 could also been detected in the northeast China and PRD by all models. M5, M8, M9, and M11 produced higher NO_2 concentrations than other models especially for M8 which also predicted very high concentrations over southeast China. Similar to NO_2, high CO concentrations were generally located over the north and central-east China as well as the east of Sichuan basin. M8, M9 and M11 produced higher CO concentrations as well. In terms of NH_3, although most models shared similar spatial patterns of NH_3 simulations, the simulated NH_3 concentrations varied largely from different models. High NH_3 concentrations were mainly located over the north China and India peninsula, which was in accordance

with the distribution of agricultural activity intensity over East Asia. Among these models, M9 and M10 produced much higher NH_3 concentrations over East Asia while M4, M5, M6, M13 and M14 produced much lower concentrations.

Figure 9 gives us more quantitative analysis of the impacts of model uncertainty on the simulations of NH_3 (9a), CO (9b) and NO_2 (9c), denoted by the spatial distribution of the standard deviation (ensemble spread), as well as the corresponding distributions of CV for each gas on the annual and seasonal basis. Note that M13 and M14 are excluded in the calculation of ensemble spread and CV to reduce the influences of the meteorological conditions and mesh sizes. It seems that the impacts of model uncertainty increase with the reactivity of the gases. NH_3 simulations were affected most by the model uncertainty, while CO suffered least from the uncertainty in the complex chemistry modeling.

The ensemble spread of NH_3 simulations exhibited a strong spatial variability with higher value mainly located in NCP. Standard deviation of the annual mean NH_3 concentrations can be over 20 ppbv in Henan province and 15 ppbv in the south of Hebei province, which is about 60–80% of the ensemble mean in Henan province and 40–60% in Hebei Province according to the CV distribution. As we mentioned in Sect. 3.1.3, these large modeling differences can be partly explained by the different treatments of the bi-directional exchange and gas-aerosol partitioning of NH_3 in different models. We can also see a strong seasonal pattern in the modeling differences of NH_3 in NCP. The ensemble spread was smallest in spring while largest in autumn, up to 25 ppbv in most areas of NCP. However, in the relative sense, the modeling differences were larger in summer and winter while less in spring and autumn. The southeast China shared similar magnitude of the ensemble spread which was about 2–5 ppbv and showed weaker seasonal variability. However, the modeling differences were larger than that in NCP in the relative sense that CV can be over 1.0 in all seasons except Summer. This can be due to that the simulated concentrations may be more influenced by the model processes over the areas with low emissions while more constrained by the local emissions over the high emission rate area.

CO was least affected by the model uncertainty among the three gases which is consistent with its weaker chemical activity and longer lifetime in the atmosphere. The ensemble spread of annual mean CO concentration was about 0.05–0.2 ppmv in the east China, only about 20%–30% of the ensemble mean. Meanwhile, CO modeling differences was more uniformly distributed in east China than NH_3 with CV less than 0.3 over most areas of east China. However, large modeling differences were visible over Myanmar during spring when there were high CO emissions from biomass burning. Modeling differences turned to be larger during winter in NCP that the ensemble spread was about 0.3–0.5 ppmv and CV about 0.3–0.4, but were still less than the modeling differences of NH_3.

NO_2 was mediumly affected by the model uncertainty among the three gases. Ensemble spread of annual mean NO_2 concentration was 5–7.5 ppbv in NCP and 2.5–5 ppbv in the southeast China, which accounted for about 20%–30% of the ensemble mean in former but more than 70% in latter. The ensemble spread was largest in winter which was over 10 ppbv in NCP (30%–40%) and 5–7.5 ppbv in southeast China (over 70%). Similar to NH_3, southeast China exhibited more modeling differences than NCP in the relative sense that CV can be over 0.7 in most areas of southeast China.

These analysis gives us a quantified result of the impact of model uncertainty on the forecast uncertainty of these gases. It indicated that for some highly active and/or short-lived primary pollutants, like NH_3, model uncertainty can also take a great

part in the forecast uncertainty besides the emission uncertainty, and further air quality data assimilation and model improvement efforts should pay special attention to such uncertainties.

4 Summary

In this study, thirteen modeling results of surface NO_2, CO and NH_3 concentrations from MICS-Asia III has been compared with each other and evaluated against the observations over NCP and PRD. Three questions are trying to be addressed which are related to the performance of current CTMs in simulating NO_2, CO and NH_3 over highly industrialized regions of China, potential factors responsible for the model deviations from observations and differences among models, as well as the impacts of model uncertainty on these gases' simulations.

Most models underpredicted NO_2 concentrations in NCP and PRD, which could be an important potential factor contributing to the overpredicted O_3 concentrations in these regions. NO_2 prediction skills were shown to be better in NCP than that in PRD with smaller biases and RMSE. Most models well reproduced the observed temporal and spatial variations of NO_2 concentrations in NCP, while relatively poor performance has been detected in PRD in terms of the spatial variations. All models significantly underestimated the CO concentrations both in NCP and PRD throughout the whole year. Such larger underestimations suggest that CO emissions were very likely to be underestimated in current emission inventories. More accurate estimate of CO emissions is needed in future studies. In contrast to the good skills in monthly variations of NO_2 and CO concentrations, a noteworthy phenomenon has been detected that all models failed to reproduce the observed monthly variation of NH_3 concentrations in NCP. Most models mismatched the observed peak and showed negative correlation coefficient, which may be closely related to the uncertainty in monthly variations of NH_3 emissions and the NH_3 gas-aerosol partitioning. Several potential factors were found to be responsible for the model deviation and differences, including chemistry-and-meteorology coupling effects, model resolutions, bi-directional exchange of NH_3 and gas-aerosol partition of NH_3, which could be the important aspects with respect to the model improvements in future. Inter-comparisons of the ensemble model quantified the impacts of model uncertainty on these gases' simulations. It shows that the impacts of model uncertainty increase with the reactivity of these gases. Models contained more uncertainties in the prediction of NH_3 than the other two gases. Based on these findings, some recommendations are made for future studies:

1) More accurate estimation of CO and NH_3 emissions are needed in future studies. Both bottom-up and top-down method (inversion technique) can help address this problem. For top-down method, advanced inversion techniques can fully take advantage of the CTMs and observations from various platforms (ground stations, satellite and radar, etc.) which has been widely used in the emission inventory estimate and correction (Miyazaki et al., 2017). However, the accuracy of emission inversion is highly subject to the model uncertainties. According to this study, NH_3 simulation was largely affected by the model uncertainties, which may cause the overcorrection of emission inventories and reduce the accuracy of emission estimate by inversion work. How to represent the model uncertainties in the current framework of emission inversion is an important aspect in future studies. Things could be better for CO considering its small and weakly spatial-dependent model uncertainties.

2) For some highly active and/or short-lived primary pollutants, like NH_3, model uncertainty can also take a great part in the forecast uncertainty. Emission uncertainty alone may not be sufficient to explain the forecast uncertainty and may cause underdispersive, and overconfident forecasts. Future studies are also needed in how to better represent the model uncertainties in the model predictions to obtain a better forecast skill.

3) Gas-aerosol partition of NH_3 is shown to be an important source of uncertainties in NH_3 simulation. The formation of NH_4^+ particles is mainly limited by the availability of H_2SO_4 and HNO_3 under ammonia-rich conditions, which involves very complex chemical reactions, including gas-phase, aqueous-phase and heterogeneous chemistry (Cheng et al., 2016;Wang et al., 2016;Zheng et al., 2015). These processes are needed to be verified and incorporated into models to better represent the chemistry in the atmosphere.

Competing interests

The authors declare that they have no conflict of interest.

Author contribution

XT, JZ, ZW and GC conducted the design of this study. JF, XW, SI, KY, TN, HL, CK, CL, LC, MZ, ZT, JL, MK, HL, BG contributed to the modelling data. ML and QW provided the emission data. KS provided the CHASER output for boundary conditions. YW, YP, GT provided the observation data. LK and XT performed the analysis and prepared the manuscript with contributions from all-authors.

Acknowledgements

This study was supported by the National Natural Science Foundation (Grant Nos. 91644216 & 41620104008), the National Key R&D Program (Grant Nos. 2018YFC0213503) and Guangdong Provincial Science and Technology Development Special Fund (No.2017B020216007). Yuepeng Pan acknowledges the National Key Research and Development Program of China (Grants 2017YFC0210100, 2016YFC0201802) and the National Natural Science Foundation of China (Grant 41405144) for financial support. We are indebted to the staff who collected the samples at the AMoN-China sites during the study period.

References

Ackermann, I. J., Hass, H., Memmesheimer, M., Ebel, A., Binkowski, F.S., and Shankar, U.: Modal aerosol dynamics model for Europe: Development and first applications, Atmos. Environ.,, 32, No.17, 2981-2999,1998.

Bergamaschi, P., Hein, R., Heimann, M., and Crutzen, P. J.: Inverse modeling of the global CO cycle 1. Inversion of CO mixing ratios, J. Geophys. Res.-Atmos., 105, 1909-1927, 10.1029/1999jd900818, 2000.

Binkowski, F.S. and Roselle, S. J.: Models 3-Community Multiscale Air Quality (CMAQ) model aerosol component:1. Model description, J. Geophys. Res.-Atmos., 108(D6), 4183, doi:10.1029/2001JD001409, 2003.

Byun, D., and Schere, K. L.: Review of the governing equations, computational algorithms, and other components of the models-3 Community Multiscale Air Quality (CMAQ) modeling system, Appl. Mech. Rev., 59, 51-77, 10.1115/1.2128636, 2006.

Carmichael, G., Sakurai, T., Streets, D., Hozumi, Y., Ueda, H., Park, S., Fung, C., Han, Z., Kajino, M., and Engardt, M.: MICS-Asia II: The model intercomparison study for Asia Phase II methodology and overview of findings, Atmos. Environ., 42, 3468-3490, 10.1016/j.atmosenv.2007.04.007, 2008.

Carmichael, G. R., Calori, G., Hayami, H., Uno, I., Cho, S. Y., Engardt, M., Kim, S. B., Ichikawa, Y., Ikeda, Y., Woo, J. H., Ueda, H., and Amann, M.: The MICS-Asia study: model intercomparison of long-range transport and sulfur deposition in East Asia, Atmos. Environ., 36, 175-199, 10.1016/s1352-2310(01)00448-4, 2002.

Carter, W. P. L.: Implementation of the SAPRC-99 Chemical Mechanism into the Models-3 Framework, Report to the United States Environmental Protection Agency, available at: http://www. engr.ucr.edu/~carter/pubs/s99mod3.pdf (last access: 6 February 2015), 2000.

Cheng, Y. F., Zheng, G. J., Wei, C., Mu, Q., Zheng, B., Wang, Z. B., Gao, M., Zhang, Q., He, K. B., Carmichael, G., Poschl, U., and Su, H.: Reactive nitrogen chemistry in aerosol water as a source of sulfate during haze events in China, Sci. Adv., 2, 11, 10.1126/sciadv.1601530, 2016.

Chin, M., Ginoux, P., Kinne, S., Torres, O., Holben, B. N., Duncan, B. N., Martin, R. V., Logan, J. A., Higurashi, A., and Nakajima, T.: Tropospheric aerosol optical thickness from the GOCART model and comparisons with satellite and Sun photometer measurements, J. Atmos. Sci., 59, 461-483, 10.1175/1520-0469(2002)059<0461:taotft>2.0.co;2, 2002.

Colella, P., and Woodward, P. L.: The piecewise parabolic method (PPM) for gas-dynamical simulations, J. Comput. Phys., 54, 174–201,1984.

Dentener, F. J., and Crutzen, P. J.: Reaction of N_2O_5 on tropospheric aerosols - impact on the global distributions of NO_x,O_3. and OH, J. Geophys. Res.-Atmos., 98, 7149-7163, 10.1029/92jd02979, 1993.

Easter, R. C., Ghan, S. J., Zhang, Y., Saylor, R. D., Chapman, E. G., Laulainen, N. S., Abdul-Razzak, H., Leung, L. R., Bian, X. D., and Zaveri, R. A.: MIRAGE: Model description and evaluation of aerosols and trace gases, J. Geophys. Res.-Atmos., 109, 46, 10.1029/2004jd004571, 2004.

Evans, M. J., and Jacob, D. J.: Impact of new laboratory studies of N_2O_5 hydrolysis on global model budgets of tropospheric nitrogen oxides, ozone, and OH, Geophys. Res. Lett., 32, 4, 10.1029/2005gl022469, 2005.

Fountoukis, C., and Nenes, A.: ISORROPIA II: a computationally efficient thermodynamic equilibrium model for K+-Ca2+-Mg2+-Nh(4)(+)-Na+-SO42--NO3--Cl--H2O aerosols, Atmos. Chem. Phys, 7, 4639-4659, 10.5194/acp-7-4639-2007, 2007.

Galmarini, S., Bianconi, R., Klug, W., Mikkelsen, T., Addis, R., Andronopoulos, S., Astrup, P., Baklanov, A., Bartniki, J., Bartzis, J. C., Bellasio, R., Bompay, F., Buckley, R., Bouzom, M., Champion, H., D'Amours, R., Davakis, E., Eleveld,

H., Geertsema, G. T., Glaab, H., Kollax, M., Ilvonen, M., Manning, A., Pechinger, U., Persson, C., Polreich, E., Potemski, S., Prodanova, M., Saltbones, J., Slaper, H., Sofiev, M. A., Syrakov, D., Sørensen, J. H., Auwera, L. V. d., Valkama, I., and Zelazny, R.: Ensemble dispersion forecasting—Part I: concept, approach and indicators, Atmos. Environ., 38, 4607-4617, https://doi.org/10.1016/j.atmosenv.2004.05.030, 2004.

Gao, M., Han, Z. W., Liu, Z. R., Li, M., Xin, J. Y., Tao, Z. N., Li, J. W., Kang, J. E., Huang, K., Dong, X. Y., Zhuang, B. L., Li, S., Ge, B. Z., Wu, Q. Z., Cheng, Y. F., Wang, Y. S., Lee, H. J., Kim, C. H., Fu, J. S. S., Wang, T. J., Chin, M. A., Woo, J. H., Zhang, Q., Wang, Z. F., and Carmichael, G. R.: Air quality and climate change, Topic 3 of the Model Inter-Comparison Study for Asia Phase III (MICS-Asia III) - Part 1: Overview and model evaluation, Atmos. Chem. Phys., 18, 4859-4884, 10.5194/acp-18-4859-2018, 2018.

Gillenwater, M.: Forgotten carbon: indirect CO_2 in greenhouse gas emission inventories, Environ. Sci. Policy, 11, 195-203, 10.1016/j.envsci.2007.09.001, 2008.

Goliff, W. S., Stockwell, W. R., Lawson, C. V.: The regional atmospheric chemistry mechanism, version 2. Atmos. Environ., 68(1),174-185, 2013.

Grell, G. A., Peckham, S. E., Schmitz, R., McKeen, S. A., Frost, G., Skamarock, W. C., and Eder, B.: Fully coupled "online" chemistry within the WRF model, Atmos. Environ., 39, 6957-6975, 10.1016/j.atmosenv.2005.04.027, 2005.

Guenther, A., Karl, T., Harley, P., Wiedinmyer, C., Palmer, P. I., and Geron, C.: Estimates of global terrestrial isoprene emissions using MEGAN (Model of Emissions of Gases and Aerosols from Nature), Atmos. Chem. Phys, 6, 3181-3210, 2006.

Han, K. M., Song, C. H., Ahn, H. J., Park, R. S., Woo, J. H., Lee, C. K., Richter, A., Burrows, J. P., Kim, J. Y., and Hong, J. H.: Investigation of NOx emissions and NOx-related chemistry in East Asia using CMAQ-predicted and GOME-derived NO2 columns, Atmos. Chem. Phys, 9, 17297-17341, 2008.

Han, Z., Sakurai, T., Ueda, H., Carmichael, G., Streets, D., Hayami, H., Wang, Z., Holloway, T., Engardt, M., and Hozumi, Y.: MICS-Asia II: Model intercomparison and evaluation of ozone and relevant species, Atmos. Environ., 42, 3491-3509, 10.1016/j.atmosenv.2007.07.031, 2008.

Hanna, S. R., Lu, Z. G., Frey, H. C., Wheeler, N., Vukovich, J., Arunachalam, S., Fernau, M., and Hansen, D. A.: Uncertainties in predicted ozone concentrations due to input uncertainties for the UAM-V photochemical grid model applied to the July 1995 OTAG domain, Atmos. Environ., 35, 891-903, 10.1016/s1352-2310(00)00367-8, 2001.

Horowitz, L. W., Walters, S., Mauzerall, D. L., Emmons, L. K., Rasch, P. J., Granier, C., Tie, X. X., Lamarque, J. F., Schultz, M. G., Tyndall, G. S., Orlando, J. J., and Brasseur, G. P.: A global simulation of tropospheric ozone and related tracers: Description and evaluation of MOZART, version 2, J. Geophys. Res.-Atmos., 108, 29, 10.1029/2002jd002853, 2003.

Hong, S. Y. : A new vertical diffusion package with an explicit treatment of entrainment processes. Mon. Weather Rev., 134(9), 2318,2006.

Husain, L., and Dutkiewicz, V. A.: A Long-term (1975-1988) study of atmospheric SO4(2-) - regional contributions and concentration trends, Atmospheric Environment Part a-General Topics, 24, 1175-1187, 10.1016/0960-1686(90)90082-x, 1990.

Janssens-Maenhout, G., Crippa, M., Guizzardi, D., Dentener, F., Muntean, M., Pouliot, G., Keating, T., Zhang, Q., Kurokawa, J., Wankmuller, R., van der Gon, H. D., Kuenen, J. J. P., Klimont, Z., Frost, G., Darras, S., Koffi, B., and Li, M.: HTAP_v2.2: a mosaic of regional and global emission grid maps for 2008 and 2010 to study hemispheric transport of air pollution, Atmos. Chem. Phys., 15, 11411-11432, 10.5194/acp-15-11411-2015, 2015.

Ji, D. S., Wang, Y. S., Wang, L. L., Chen, L. F., Hu, B., Tang, G. Q., Xin, J. Y., Song, T., Wen, T. X., Sun, Y., Pan, Y. P., and Liu, Z. R.: Analysis of heavy pollution episodes in selected cities of northern China, Atmos. Environ., 50, 338-348, 10.1016/j.atmosenv.2011.11.053, 2012.

Jin, X. M., and Holloway, T.: Spatial and temporal variability of ozone sensitivity over China observed from the Ozone Monitoring Instrument, J. Geophys. Res.-Atmos., 120, 7229-7246, 10.1002/2015jd023250, 2015.

Kajino, M., Inomata, Y., Sato, K., Ueda, H., Han, Z., An, J., Katata, G., Deushi, M., Maki, T., Oshima, N., Kurokawa, J., Ohara, T., Takami, A., and Hatakeyama, S.: Development of the RAQM2 aerosol chemical transport model and predictions of the Northeast Asian aerosol mass, size, chemistry, and mixing type, Atmos. Chem. Phys., 12, 11833-11856, 10.5194/acp-12-11833-2012, 2012.

Kajino, M., Deushi, M., Sekiyama, T. T., Oshima, N., Yumimoto, K., Tanaka, T. Y., Ching, J., hashimoto, Ak., Yamamoto, T., Ikegami, M., Kamada, A., Miyashita, M., Inomata, Y., Shima, S., Adachi, K., Zaizen, Y., Igarashi, Y., Ueda, H., Maki, T., and Mikami, M., NHM-Chem, the Japan Meteorological Agency's regional meteorology - chemistry model (v1.0): model description and aerosol representations, Geosci. Model Dev. Discuss, in review, doi:10.5194/gmd-2018-128, 2018.

Khoder, M. I.: Atmospheric conversion of sulfur dioxide to particulate sulfate and nitrogen dioxide to particulate nitrate and gaseous nitric acid in an urban area, Chemosphere, 49, 675-684, 10.1016/s0045-6535(02)00391-0, 2002.

Kurokawa, J., Ohara, T., Morikawa, T., Hanayama, S., Janssens-Maenhout, G., Fukui, T., Kawashima, K., and Akimoto, H.: Emissions of air pollutants and greenhouse gases over Asian regions during 2000-2008: Regional Emission inventory in ASia (REAS) version 2, Atmos. Chem. Phys., 13, 11019-11058, 10.5194/acp-13-11019-2013, 2013.

Lelieveld, J., Evans, J. S., Fnais, M., Giannadaki, D., and Pozzer, A.: The contribution of outdoor air pollution sources to premature mortality on a global scale, Nature, 525, 367-+, 10.1038/nature15371, 2015.

Levy, H.: NORMAL ATMOSPHERE - LARGE RADICAL AND FORMALDEHYDE CONCENTRATIONS PREDICTED, Science, 173, 141-&, 10.1126/science.173.3992.141, 1971.

Li, M., Zhang, Q., Kurokawa, J. I., Woo, J. H., He, K., Lu, Z., Ohara, T., Song, Y., Streets, D. G., Carmichael, G. R., Cheng, Y., Hong, C., Huo, H., Jiang, X., Kang, S., Liu, F., Su, H., and Zheng, B.: MIX: a mosaic Asian anthropogenic emission inventory under the international collaboration framework of the MICS-Asia and HTAP, Atmos. Chem. Phys., 17, 935-963, 10.5194/acp-17-935-2017, 2017.

Li, J., Nagashima, T., Kong, L., Ge, B., Yamaji, K., Fu, J. S., Wang, X., Fan, Q., Itahashi, S., Lee, H. J., Kim, C. H., Lin, C. Y., Zhang, M., Tao, Z., Kajino, M., Liao, H., Li, M., Woo, J. H., Kurokawa, J. I., Wu, Q., Akimoto, H., Carmichael, G. R., and Wang, Z.: Model evaluation and inter-comparison of surface-level ozone and relevant species in East Asia in the context of MICS-Asia phase III Part I: overview, Atmos. Chem. Phys. Discuss., 2019, 1-56, 10.5194/acp-2018-1283, 2019.

Lin, J. T., and McElroy, M. B.: Impacts of boundary layer mixing on pollutant vertical profiles in the lower troposphere: Implications to satellite remote sensing, Atmos. Environ., 44, 1726-1739, 10.1016/j.atmosenv.2010.02.009, 2010.

Mallet, V., and Sportisse, B.: Uncertainty in a chemistry-transport model due to physical parameterizations and numerical approximations: An ensemble approach applied to ozone modeling, J. Geophys. Res.-Atmos., 111, 15, 10.1029/2005jd006149, 2006.

Martin, R. V., Jacob, D. J., Logan, J. A., Bey, I., Yantosca, R. M., Staudt, A. C., Li, Q., Fiore, A. M., Duncan, B. N., and Liu, H.: Interpretation of TOMs observations of tropical tropospheric ozone with a global model and in situ observations, J. Geophys. Res.-Atmos, 107(D18), ACH 4-1–ACH 4-27, 2002.

Meng, Z. Y., Lin, W. L., Jiang, X. M., Yan, P., Wang, Y., Zhang, Y. M., Jia, X. F., and Yu, X. L.: Characteristics of atmospheric ammonia over Beijing, China, Atmos. Chem. Phys., 11, 6139-6151, 10.5194/acp-11-6139-2011, 2011.

Miyazaki, K., Eskes, H. J., Sudo, K., Takigawa, M., Weele, M. V., and Boersma, K. F.: Simultaneous assimilation of satellite NO_2, O_3, CO, and HNO_3 data for the analysis of tropospheric chemical composition and emissions, Atmospheric Chemistry & Physics & Discussions, 264, 1017-1023, 2012.

Miyazaki, K., Eskes, H., Sudo, K., Boersma, K. F., Bowman, K., and Kanaya, Y.: Decadal changes in global surface NO_x emissions from multi-constituent satellite data assimilation, Atmos. Chem. Phys., 17, 807-837, 10.5194/acp-17-807-2017, 2017.

Nemitz, E., Milford, C., and Sutton, M. A.: A two-layer canopy compensation point model for describing bi-directional biosphere-atmosphere exchange of ammonia, Q. J. R. Meteorol. Soc., 127, 815-833, 10.1256/smsqj.57305, 2001.

Nenes, A., Pandis, S.N., Pilinis, C.: ISORROPIA: A new thermodynamic equilibrium model for multiphase multicomponent inorganic aerosols, Aquat. Geoch., 4, 123-152,1998.

Noije, T. P. C. V., Eskes, H. J., Dentener, F. J., Stevenson, D. S., Ellingsen, K., Schultz, M. G., Wild, O., Amann, M., Atherton, C. S., and Bergmann, D. J.: Multi-model ensemble simulations of tropospheric NO_2 compared with GOME retrievals for the year 2000, Atmos. Chem. Phys., 6, 2943-2979, 2006.

Novelli, P. C., Masarie, K. A., and Lang, P. M.: Distributions and recent changes of carbon monoxide in the lower troposphere, J. Geophys. Res.-Atmos., 103, 19015-19033, 10.1029/98jd01366, 1998.

Pan, Y., Tian, S., Zhao, Y., Zhang, L., Zhu, X., Gao, J., Huang, W., Zhou, Y., Song, Y., Zhang, Q., and Wang, Y.: Identifying ammonia hotspots in China using a national observation network, Environmental Science & Technology, 10.1021/acs.est.7b05235, 2018.

Pan, Y. P., Wang, Y. S., Tang, G. Q., and Wu, D.: Wet and dry deposition of atmospheric nitrogen at ten sites in Northern China, Atmos. Chem. Phys., 12, 6515-6535, 10.5194/acp-12-6515-2012, 2012.

Peters-Lidard, C. D., Kemp, E. M., Matsui, T., Santanello, J. A., Kumar, S. V., Jacob, J. P., Clune, T., Tao, W. K., Chin, M., Hou, A., Case, J. L., Kim, D., Kim, K. M., Lau, W., Liu, Y. Q., Shi, J., Starr, D., Tan, Q., Tao, Z. N., Zaitchik, B. F., Zavodsky, B., Zhang, S. Q., and Zupanski, M.: Integrated modeling of aerosol, cloud, precipitation and land processes at satellite-resolved scales, Environmental Modelling & Software, 67, 149-159, 10.1016/j.envsoft.2015.01.007, 2015.

Petron, G., Granier, C., Khattatov, B., Lamarque, J. F., Yudin, V., Muller, J. F., and Gille, J.: Inverse modeling of carbon monoxide surface emissions using Climate Monitoring and Diagnostics Laboratory network observations, J. Geophys. Res.-Atmos., 107, 23, 10.1029/2001jd001305, 2002.

Petron, G., Granier, C., Khattatov, B., Yudin, V., Lamarque, J. F., Emmons, L., Gille, J., and Edwards, D. P.: Monthly CO surface sources inventory based on the 2000-2001 MOPITT satellite data, Geophys. Res. Lett., 31, 5, 10.1029/2004gl020560, 2004.

Pielke, R. A., Cotton, W. R., Walko, R. L., Tremback, C. J., Lyons, W. A., Grasso, L. D., Nicholls, M. E., Moran, M. D., Wesley, D. A., Lee, T. J., and Copeland, J. H.: A comprehensive meteorological modeling system - RAMS, Meteorol. Atmos. Phys., 49, 69-91, 10.1007/bf01025401, 1992.

Pleim, J. E., Xiu, A., Finkelstein, P. L., and Otte, T. L.: A Coupled Land-Surface and Dry Deposition Model and Comparison to Field Measurements of Surface Heat, Moisture, and Ozone Fluxes, Water Air Soil Poll., 1, 243–252, 2001.

Pleim, J. E.: A combined local and nonlocal closure model for the atmospheric boundary layer, Part I: Model description and testing, J. Appl. Meteor. Climatol., 46, 1383–1395, 2007.

Randerson, J. T., Werf, G. R. v. d., Giglio, L., Collatz, G. J., and Kasibhatla, P. S.: Global Fire Emissions Database, Version 3 (GFEDv3.1). Data set. Available on-line [http://daac.ornl.gov/] from Oak Ridge National Laboratory Distributed Active Archive Center, Oak Ridge, Tennessee, USA. doi:10.3334/ORNLDAAC/1191, 2013.

Rao, S. T., Galmarini, S., and Puckett, K.: Air Quality Model Evaluation International Initiative (AQMEII) Advancing the State of the Science in Regional Photochemical Modeling and Its Applications, Bull. Amer. Meteorol. Soc., 92, 23-30, 10.1175/2010bams3069.1, 2011.

Saito, K., Fujita, T., Yamada, Y., Ishida, J. I., Kumagai, Y., Aranami, K., Ohmori, S., Nagasawa, R., Kumagai, S., Muroi, C., Kato, T., Eito, H., and Yamazaki, Y.: The operational JMA nonhydrostatic mesoscale model, Mon. Weather Rev., 134, 1266-1298, 10.1175/mwr3120.1, 2006.

Shao, M., Zhang, Y. H., Zeng, L. M., Tang, X. Y., Zhang, J., Zhong, L. J., and Wang, B. G.: Ground-level ozone in the Pearl River Delta and the roles of VOC and NOx in its production, J. Environ. Manage., 90, 512-518, 10.1016/j.jenvman.2007.12.008, 2009.

Shen, J. L., Liu, X. J., Zhang, Y., Fangmeier, A., Goulding, K., and Zhang, F. S.: Atmospheric ammonia and particulate ammonium from agricultural sources in the North China Plain, Atmos. Environ., 45, 5033-5041, 10.1016/j.atmosenv.2011.02.031, 2011.

Sillman, S.: The relation between ozone, NOx and hydrocarbons in urban and polluted rural environments, Atmos. Environ., 33, 1821-1845, 10.1016/s1352-2310(98)00345-8, 1999.

Skamarock, W. C.: A description of the advanced research WRF version 3, Ncar Technical, 113, 7--25, 2008.

Stein, O., Schultz, M. G., Bouarar, I., Clark, H., Huijnen, V., Gaudel, A., George, M., and Clerbaux, C.: On the wintertime low bias of Northern Hemisphere carbon monoxide found in global model simulations, Atmos. Chem. Phys., 14, 9295-9316, 10.5194/acp-14-9295-2014, 2014.

Steinfeld, J. I.: Atmos. Chem. Phys.: From Air Pollution to Climate Change, Wiley, 1595-1595 pp., 1998.

Stockwell, W. R., Middleton, P., Chang, J. S. and Tang, X.: The second generation regional Acid Deposition Model chemical mechanism for regional air quality modeling, J. Geophys. Res., 95, 16,343-16,367, 1990.

Sudo, K., Takahashi, M., Kurokawa, J., and Akimoto, H.: CHASER: A global chemical model of the troposphere - 1. Model description, J. Geophys. Res.-Atmos., 107, 20, 10.1029/2001jd001113, 2002a

Sudo, K., Takahashi, M., and Akimoto, H.: CHASER: A global chemical model of the troposphere - 2 . Model results and evaluation, J. Geophys. Res.-Atmos., 107, 39, 10.1029/2001jd001114, 2002b

Sun, Y. L., Wang, Z. F., Dong, H. B., Yang, T., Li, J., Pan, X. L., Chen, P., and Jayne, J. T.: Characterization of summer organic and inorganic aerosols in Beijing, China with an Aerosol Chemical Speciation Monitor, Atmos. Environ., 51, 250-259, 10.1016/j.atmosenv.2012.01.013, 2012.

Sun, Y. L., Wang, Z. F., Fu, P. Q., Yang, T., Jiang, Q., Dong, H. B., Li, J., and Jia, J. J.: Aerosol composition, sources and processes during wintertime in Beijing, China, Atmos. Chem. Phys., 13, 4577-4592, 10.5194/acp-13-4577-2013, 2013.

Tang, G., Wang, Y., Li, X., Ji, D., Hsu, S., and Gao, X.: Spatial-temporal variations in surface ozone in Northern China as observed during 2009-2010 and possible implications for future air quality control strategies, Atmos. Chem. Phys., 12, 2757-2776, 10.5194/acp-12-2757-2012, 2012

Tang, X., Zhu, J., Wang, Z. F., Wang, M., Gbaguidi, A., Li, J., Shao, M., Tang, G. Q., and Ji, D. S.: Inversion of CO emissions over Beijing and its surrounding areas with ensemble Kalman filter, Atmos. Environ., 81, 676-686, 10.1016/j.atmosenv.2013.08.051, 2013.

Tao, Z., Santanello, J.A., Chin, M., Zhou, S., Tan, Q., Kemp, E.M., and Peters-Lidard, C. D.: Effect of land cover on atmospheric processes and air quality over the continental United States – A NASA Unifed WRF (NU-WRF) model study. Atmos. Chem. Phys., 13, 6207-6226, doi:10.5194/acp-13-6207-203, 2013.

Uno, I., He, Y., Ohara, T., Yamaji, K., Kurokawa, J. I., Katayama, M., Wang, Z., Noguchi, K., Hayashida, S., Richter, A., and Burrows, J. P.: Systematic analysis of interannual and seasonal variations of model-simulated tropospheric NO_2 in Asia and comparison with GOME-satellite data, Atmos. Chem. Phys., 7, 1671-1681, 10.5194/acp-7-1671-2007, 2007.

US EPA Office of Research and Development: CMAQv5.0, , doi:10.5281/zenodo.1079888, 2012.

von Bobrutzki, K., Braban, C. F., Famulari, D., Jones, S. K., Blackall, T., Smith, T. E. L., Blom, M., Coe, H., Gallagher, M., Ghalaieny, M., McGillen, M. R., Percival, C. J., Whitehead, J. D., Ellis, R., Murphy, J., Mohacsi, A., Pogany, A.,

Junninen, H., Rantanen, S., Sutton, M. A., and Nemitz, E.: Field inter-comparison of eleven atmospheric ammonia measurement techniques, Atmos. Meas. Tech., 3, 91-112, 10.5194/amt-3-91-2010, 2010

Walcek, C. J. and Teylor, G. R.: A theoretical method for computing vertical distributions of acidity and sulfate production within cumulus clouds, J. Atmos. Sci., 43, 339–355, 1986.

Wang, G., Zhang, R., Gomez, M. E., Yang, L., Zamora, M. L., Hu, M., Lin, Y., Peng, J., Guo, S., and Meng, J.: Persistent sulfate formation from London Fog to Chinese haze, Proceedings of the National Academy Ofences of the United States of America, 113, 13630, 2016.

Wang, Z. F., Maeda, T., Hayashi, M., Hsiao, L. F., and Liu, K. Y.: A nested air quality prediction modeling system for urban and regional scales: Application for high-ozone episode in Taiwan, Water Air Soil Pollut., 130, 391-396, 10.1023/a:1013833217916, 2001.

Warner, J. X., Wei, Z., Strow, L. L., Dickerson, R. R., and Nowak, J. B.: The global tropospheric ammonia distribution as seen in the 13-year AIRS measurement record, Atmos. Chem. Phys., 16, 5467-5479, 10.5194/acp-16-5467-2016, 2016.

Warner, J. X., Dickerson, R. R., Wei, Z., Strow, L. L., Wang, Y., and Liang, Q.: Increased atmospheric ammonia over the world's major agricultural areas detected from space, Geophys. Res. Lett., 44, 2875-2884, 10.1002/2016gl072305, 2017.

Xu, W., Wu, Q. H., Liu, X. J., Tang, A. H., Dore, A., and Heal, M.: Characteristics of ammonia, acid gases, and PM2.5 for three typical land-use types in the North China Plain, Environ. Sci. Pollut. Res., 23, 1158-1172, 10.1007/s11356-015-5648-3, 2016.

Yamartino, R. J.: Nonnegative, conserved scalar transport using grid-cell-centered, spectrally constrained Blackman cubics for applications on a variable-thickness mesh, Mon. Weather Rev., 121, 753–763, 1993

Yarwood, G., Rao, S., Yocke, M., Whitten, G.: Updates to the Carbon Bond Chemical Mechanism: CB05 Final Report to the US EPA, RT-0400675,2005.

Wesely, M. L.: Parameterization of surface resistances to gaseous dry deposition in regional-scale numerical models, Atmos. Envion., 23(6), 1293-1304, 1989.

Zaveri, R, A,, Peters, L. K.: A new lumped structure photochemical mechanism for large-scale applications. J. Geophys. Res.104, 30387-30415,1999.

Zhang, L., Brook, J. L., and Vet, R.: A revised parameterization for gaseous dry deposition in air-quality models, Atmos. Chem. Phys., 3, 2067-2082, 2003.

Zhang, L., Chen, Y. F., Zhao, Y. H., Henze, D. K., Zhu, L. Y., Song, Y., Paulot, F., Liu, X. J., Pan, Y. P., Lin, Y., and Huang, B. X.: Agricultural ammonia emissions in China: reconciling bottom-up and top-down estimates, Atmos. Chem. Phys., 18, 339-355, 10.5194/acp-18-339-2018, 2018.

Zheng, B., Zhang, Q., Zhang, Y., He, K. B., Wang, K., Zheng, G. J., Duan, F. K., Ma, Y. L., and Kimoto, T.: Heterogeneous chemistry: a mechanism missing in current models to explain secondary inorganic aerosol formation during the January 2013 haze episode in North China, Atmos. Chem. Phys., 15, 2031-2049, 10.5194/acp-15-2031-2015, 2015.

Zhong, L. J., Louie, P. K. K., Zheng, J. Y., Wai, K. M., Ho, J. W. K., Yuan, Z. B., Lau, A. K. H., Yue, D. L., and Zhou, Y.: The Pearl River Delta Regional Air Quality Monitoring Network - Regional Collaborative Efforts on Joint Air Quality Management, Aerosol Air Qual. Res., 13, 1582-U1232, 10.4209/aaqr.2012.10.0276, 2013.

Atmos. Chem. Phys. Discuss., https://doi.org/10.5194/acp-2018-1158
Manuscript under review for journal Atmos. Chem. Phys.
Discussion started: 6 May 2019

Atmospheric Chemistry and Physics Discussions

Tables

Table 1: Basic configurations of participating modeling systems in MICS-Asia III

No	Horizontal resolution	Vertical resolution	First layer height	Horizontal advection	Vertical advection	Horizontal Diffusion	Vertical Diffusion	Gas phase chemistry	Aerosol processes	Dry depositiono f gases	Wet deposition of gases	Meteorology	Boundary condition	Online (Yes or No)
M1	45km	40σ_p level	57 m	Yamo (Yamartino, 1993)	ppm (Collella and Woodward, 1984)	multiscale	ACM2 (Pleim, 2007)	SAPRC99 (Carter, 2000)	Aero6 (Binkowski and Roselle, 2003)	Wesely (1989)	Henry's law	Standard[a]	GEOS-Chem (Martin et al., 2002)	No
M2	45km	40σ_p level	57 m	Yamo	ppm	multiscale	ACM2	SAPRC99	Aero6	Wesely (1989)	Henry's law	Standard[a]	Default	No
M3	45km	40σ_p level	57 m	Yamo	Yamo	multiscale	ACM2	CB05 (Yarwood et al., 2005)	Aero5	Wesely (1989)	Henry's law	Standard[a]	GEOS-Chem	No
M4	45km	40σ_p level	57 m	ppm	ppm	multiscale	ACM2_ inline	SAPRC99	Aero5	Wesely (1989)	Henry's law	Standard[a]	CHASER (Sudo et al., 2002a)	No
M5	45km	40σ_p level	57 m	ppm	ppm	multiscale	ACM2_ inline	SAPRC99	Aero5	M3DRY (Pleim et al., 2001)	Henry's law	Standard[a]	CHASER	No
M6	45km	40σ_p level	57 m	Yamo	Yamo	multiscale	ACM2_ inline	SAPRC99	Aero5	M3DRY	ACM	Standard[a]	CHASER	No
M7	45km	40σ_p level	29 m	Monotonic	Monotonic	no diffusion	no diffusion	RACM-ESRL with KPP (Goliff et al.,2013)	MADE (Ackerman n et al., 1998)	Wesely (1989)	Henry's law	WRF/NCEP[a]	Default	No
M8	45km	40σ_p level	57 m	5th order Monotonic	3th order Monotonic	MYJ	MYJ	RACM with KPP	MADE	Wesely (1989)	AQCHEM	WRF/NCEP[a]	CHASER	Yes
M9	45km	40σ_p level	16 m	5th order Monotonic	3th order Monotonic	Smagorinsk y first order closure	YSU (Hong et al., 2006)	RADM2 (Stockwell et al., 1990)	MADE	Wesely (1989)	Easter et al., (2004)	WRF/NCEP[a]	GEOS-Chem	Yes
M10	45km	60σ_p level	44 m	Monotonic	3th order Monotonic	2th order Monotonic	YSU	RADM2	GOCART	Wesely (1989)	Grell	WRF/ MERRA2[a]	MOZART + GOCART[b]	No
M11	45km	20σ_z level	50 m	Walcek and Aleksic (1998)	Walcek and Aleksic (1998)	multicale	K-theory	CBMZ (Zaveri et al.,1999)	ISORROPI A1.7 (Nenes et al.,1998)	Wesely (1989)	Henry's law	Standard[a]	CHASER	No

Atmos. Chem. Phys. Discuss., https://doi.org/10.5194/acp-2018-1158
Manuscript under review for journal Atmos. Chem. Phys.
Discussion started: 6 May 2019

Atmospheric Chemistry and Physics Discussions

M12	45km	40 σ_p level	54 m	Walcek and Aleksic (1998)	Walcek and Aleksic (1998)	FTCS	FTCS	SAPRC99	Kajino et al. (2012)	Zhang et al. (2003)	Henry's law	Standard[a]	CHASER	No
M13	0.5°×0.667°	47σ_p level	60 m	ppm	Huynh/Van Leer/Lin full monotonicity constraint	Lin and McElroy, 2010	Lin and McElroy, 2010	Tropchem	ISORROPI A2.0 (Fountoukis and Nenes, 2007)	Wesely	Henry's law	GEOS-5[a]	Geos-Chem	No
M14	64km	15σ_z level	100 m	ppm	ppm	multiscale	ACM2	SAPRC99	ISORROPI A1.7	Wesely (1989)	Henry's law	RAMS/NCEP[a]	Geos-Chem	No

[a] Standard represents the reference meteorological field provided by MICS-Asia III project; WRF/NCEP and WRF/MERRA represents the meteorological field of the participating model itself, which was run by WRF driven by the NCEP and Modern Era Retrospective-analysis for Research and Applications (MERRA) reanalysis dataset. RAMS/NCEP is the meteorology field run by RAMS driven by the NCEP reanalysis dataset.

[b] Boundary conditions of M10 are from MOZART and GOCART (Chin et al., 2002; Horowitz et al.,2003), which provided results for gaseous pollutants and aerosols, respectively.

Atmos. Chem. Phys. Discuss., https://doi.org/10.5194/acp-2018-1158
Manuscript under review for journal Atmos. Chem. Phys.
Discussion started: 6 May 2019

Atmospheric Chemistry and Physics Discussions

Table 2: Statistics of simulated annual mean concentrations sampled from different sites in NCP and PRD.

Species	Regions	Statistics	Model													
			M1	M2	M4	M5	M6	M7	M8	M9	M10	M11	M12	M13	M14	Ense
NO_2	NCP	R(spatial)[a]	0.63	0.67	0.67	0.67	0.67	0.70	0.70	0.59	0.57	0.66	0.69	-	0.70	0.67
		R(temporal)[b]	0.82	0.92	0.93	0.86	0.92	0.81	0.28	0.85	0.95	0.75	0.90	-	0.96	0.91
		MBE	-4.11	-5.66	-6.54	1.86	-5.12	-5.04	3.30	8.28	-2.45	0.00	-3.81	-	-2.99	-1.86
		NMB(%)	-17.8	-24.5	-28.4	8.0	-22.2	-21.9	14.2	35.9	-10.6	0.02	-16.5	-	-13.0	-8.0
		RMSE	7.40	8.25	8.79	6.75	8.01	7.55	6.54	12.74	7.72	6.37	7.38	-	6.68	6.36
	PRD	R(spatial) [a]	0.12	0.06	0.07	0.07	0.06	0.12	0.20	0.38	0.00	0.08	0.12	-	0.02	0.10
		R(temporal)[b]	0.93	0.80	0.86	0.88	0.79	0.68	0.83	0.95	0.74	0.74	0.75	-	0.52	0.86
		MBE	-6.73	-9.84	-7.21	1.96	-6.66	-3.99	3.24	-7.61	-1.84	3.02	-5.49	-	-5.03	-3.85
		NMB(%)	-30.1	-44.0	-32.3	8.8	-29.8	-17.9	14.5	-34.0	-8.2	13.5	-24.6	-	-22.5	-17.2
		RMSE	11.31	13.14	12.00	10.80	11.84	10.60	8.73	10.69	10.72	10.51	11.68	-	12.00	10.15
CO	NCP	R(spatial) [a]	0.35	0.48	0.27	0.34	0.36	0.22	0.19	0.48	0.49	0.33	0.35	-0.13	0.29	0.37
		R(temporal)[b]	0.94	0.96	0.92	0.22	0.90	0.77	0.94	0.92	0.82	0.85	0.94	0.85	0.88	0.92
		MBE	-1.53	-1.35	-1.59	-1.69	-1.52	-1.64	-1.29	-1.16	-1.55	-1.37	-1.38	-1.53	-1.51	-1.47
		NMB(%)	-68.9	-60.9	-71.4	-76.2	-68.2	-73.7	-58.2	-52.0	-70.0	-61.6	-62.3	-68.9	-68.0	-66.2
		RMSE	1.71	1.54	1.77	1.86	1.70	1.82	1.51	1.36	1.74	1.57	1.58	1.74	1.70	1.66
	PRD	R(spatial) [a]	0.04	-0.24	-0.25	-0.23	-0.22	-0.05	0.08	0.55	-0.02	-0.01	-0.22	0.09	-0.21	-0.06
		R(temporal)[b]	0.96	0.91	0.93	0.84	0.95	0.90	0.90	0.96	0.83	0.87	0.93	0.76	0.82	0.94
		MBE	-0.66	-0.64	-0.65	-0.64	-0.62	-0.64	-0.51	-0.57	-0.50	-0.51	-0.58	-0.52	-0.67	-0.59
		NMB(%)	-68.4	-67.0	-67.0	-66.7	-64.7	-66.5	-53.3	-59.7	-52.3	-52.7	-60.7	-54.1	-69.6	-61.7
		RMSE	0.70	0.70	0.70	0.69	0.67	0.69	0.57	0.62	0.56	0.57	0.64	0.58	0.72	0.65
NH_3	NCP	R(spatial)[a]	0.72	0.70	0.69	0.70	0.71	0.65	-	0.70	0.57	0.62	0.67	0.61	0.58	0.69
		R(temporal)[b]	-0.48	-0.22	-0.45	-0.55	-0.41	0.04	-	-0.19	0.64	0.08	-0.37	0.65	-0.04	-0.17
		MBE	-0.69	2.95	-6.14	-6.61	-3.89	4.94	-	21.8	10.5	-0.07	0.31	-5.19	-12.2	0.47
		NMB(%)	-3.8	16.1	-33.5	-36.0	-21.2	26.9	-	118.7	57.1	-0.4	1.69	-28.3	-66.3	2.59
		RMSE	7.20	10.04	8.95	9.24	7.48	8.78	-	29.24	13.48	8.30	7.33	8.82	14.48	7.20

[a] R(spatial) represents the spatial correlation coefficients between simulated and observed concentrations sampled from different stations in NCP or PRD;

[b] R(temporal) represents the temporal correlation coefficients between simulated and observed monthly mean concentrations from January to December in 2010;

Atmos. Chem. Phys. Discuss., https://doi.org/10.5194/acp-2018-1158
Manuscript under review for journal Atmos. Chem. Phys.
Discussion started: 6 May 2019

Atmospheric Chemistry and Physics Discussions

Figures

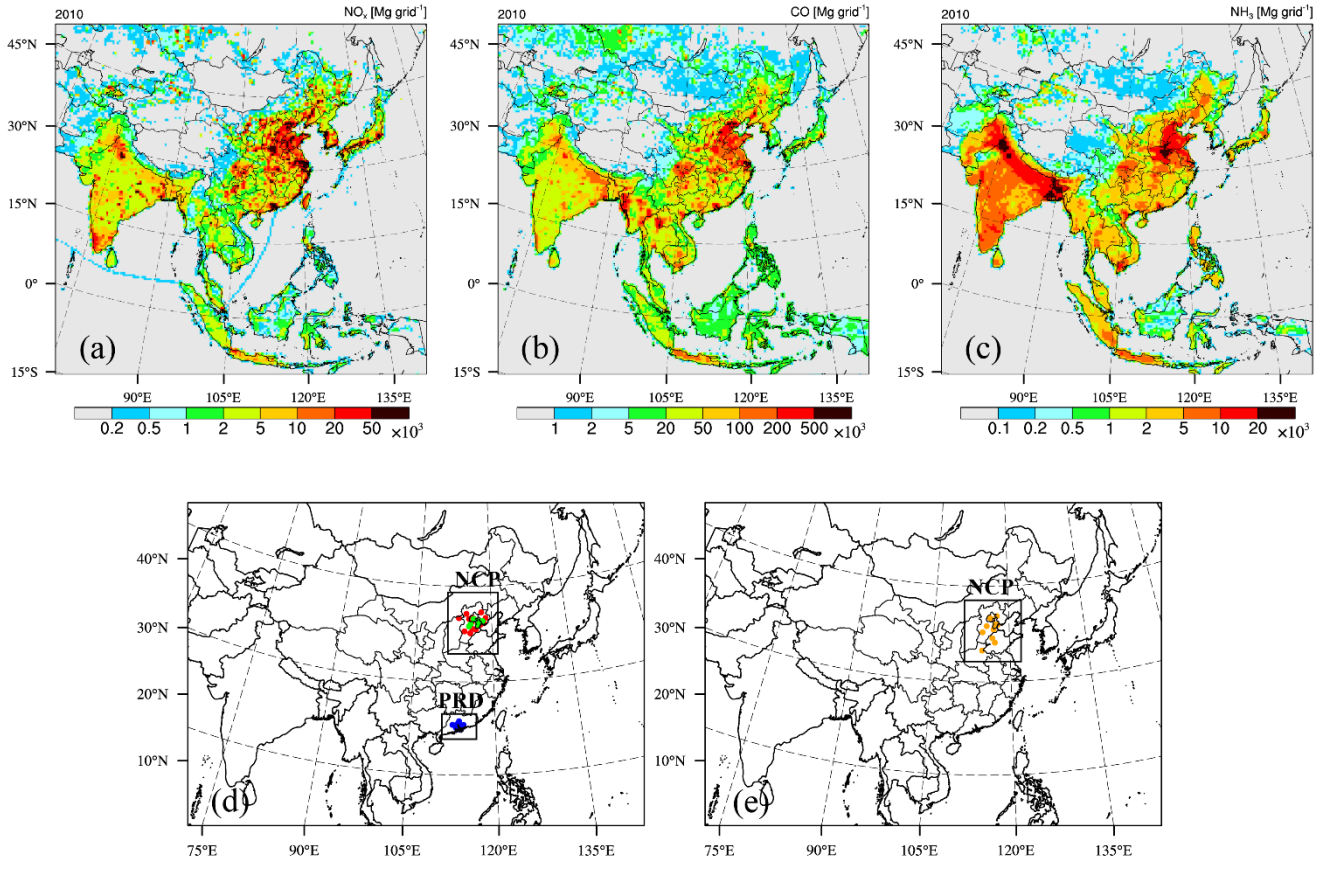

Figure 1: Modeling domains of the participated models except M13 and M14 along with spatial distributions of the total emissions of (a) NO_x, (b) CO and (c) NH_3 in 2010 provided by MICS-Asia III (upper panel), and the distributions of observation stations of (d) NO_2 and CO over NCP and PRD, as well as (e) NH_3 over NCP (lower panel). The horizontal resolution is 45km×45km. Note that domains of M13 and M14 are shown in fig. 7 and only six of nineteen observational sites (blue) over NCP have CO measurements.

Atmos. Chem. Phys. Discuss., https://doi.org/10.5194/acp-2018-1158
Manuscript under review for journal Atmos. Chem. Phys.
Discussion started: 6 May 2019

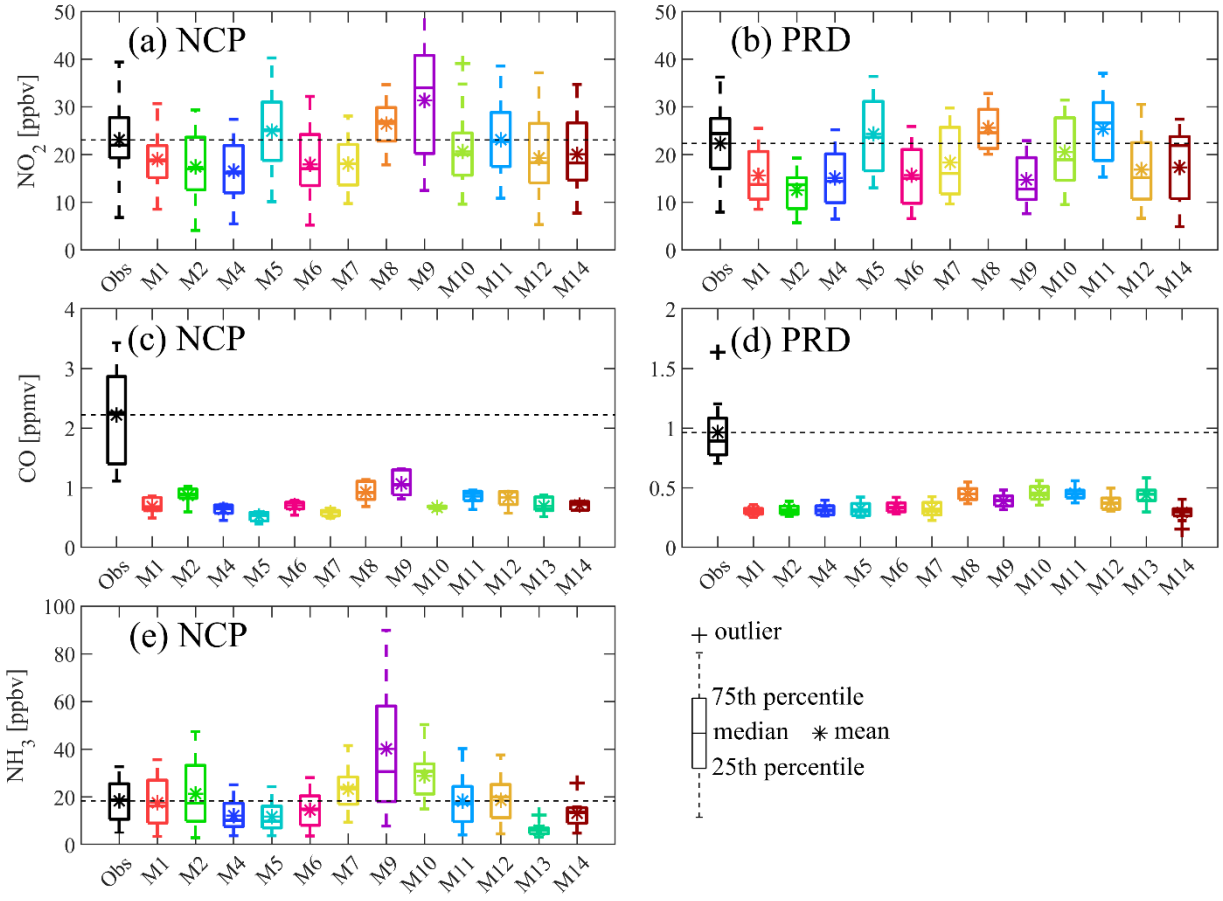

Figure 2: Boxplot of simulated and observed annual mean NO_2, CO and NH_3 concentrations sampled from different stations over NCP (a, c, e) and PRD (b, d). The outlier was defined as values larger than $q_3 + 1.5 \times (q_3 - q_1)$ or less than $q_1 - 1.5 \times (q_3 - q_1)$, where q_3 denotes the 75th percentile, and q_1 the 25th percentile. This approximately corresponds to 99.3 percent coverage if the data are normally distributed.

Atmos. Chem. Phys. Discuss., https://doi.org/10.5194/acp-2018-1158
Manuscript under review for journal Atmos. Chem. Phys.
Discussion started: 6 May 2019

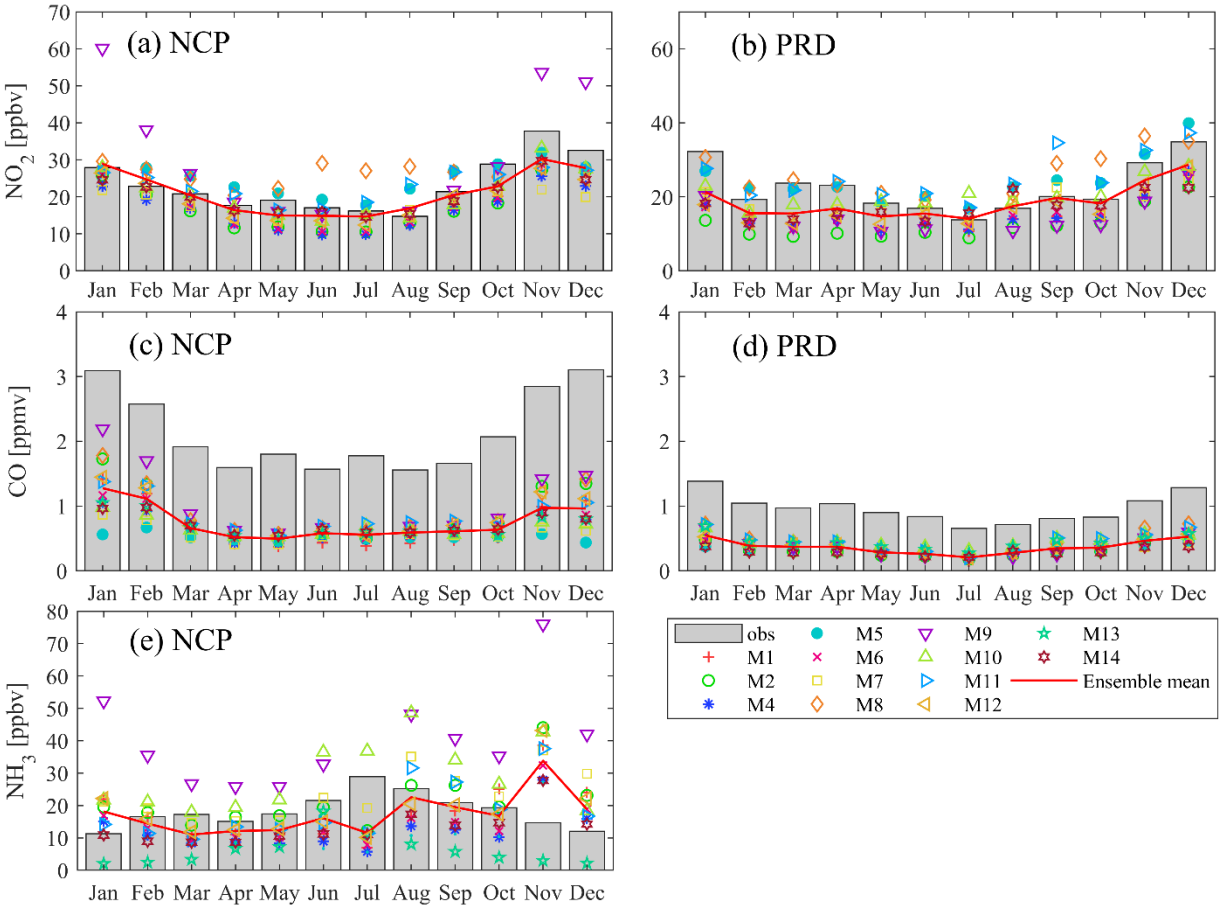

Figure 3: Timeseries of regional mean NO_2, CO concentrations over NCP (a, c) and PRD (b, d) as well as NH_3 concentrations over NCP (e) from January to December in year 2010.

Atmos. Chem. Phys. Discuss., https://doi.org/10.5194/acp-2018-1158
Manuscript under review for journal Atmos. Chem. Phys.
Discussion started: 6 May 2019

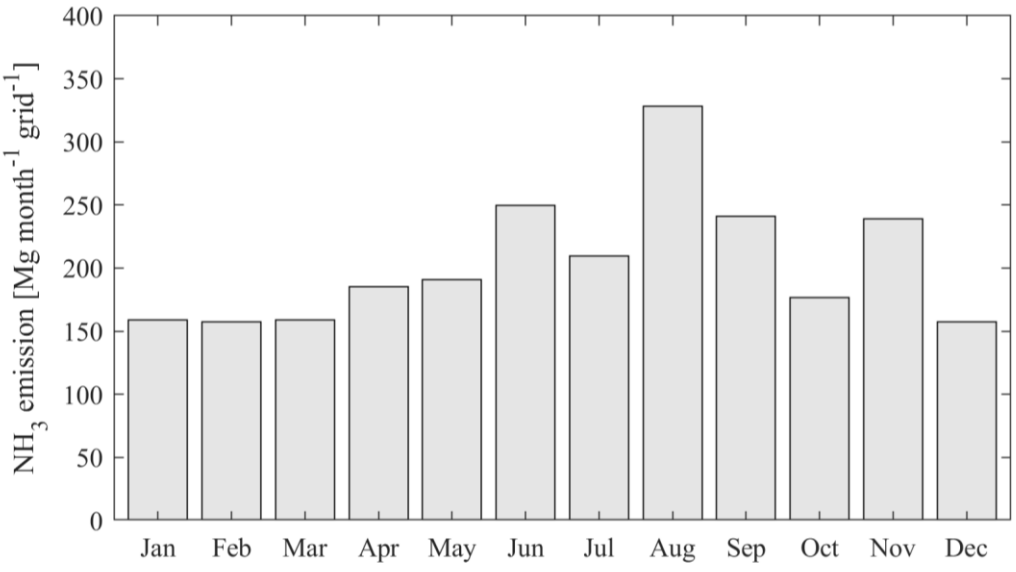

Figure 4: Timeseries of NH_3 emissions over NCP provided by MICS-Asia III on a horizontal resolution of 45km×45km from January to December in year 2010.

Atmos. Chem. Phys. Discuss., https://doi.org/10.5194/acp-2018-1158
Manuscript under review for journal Atmos. Chem. Phys.
Discussion started: 6 May 2019

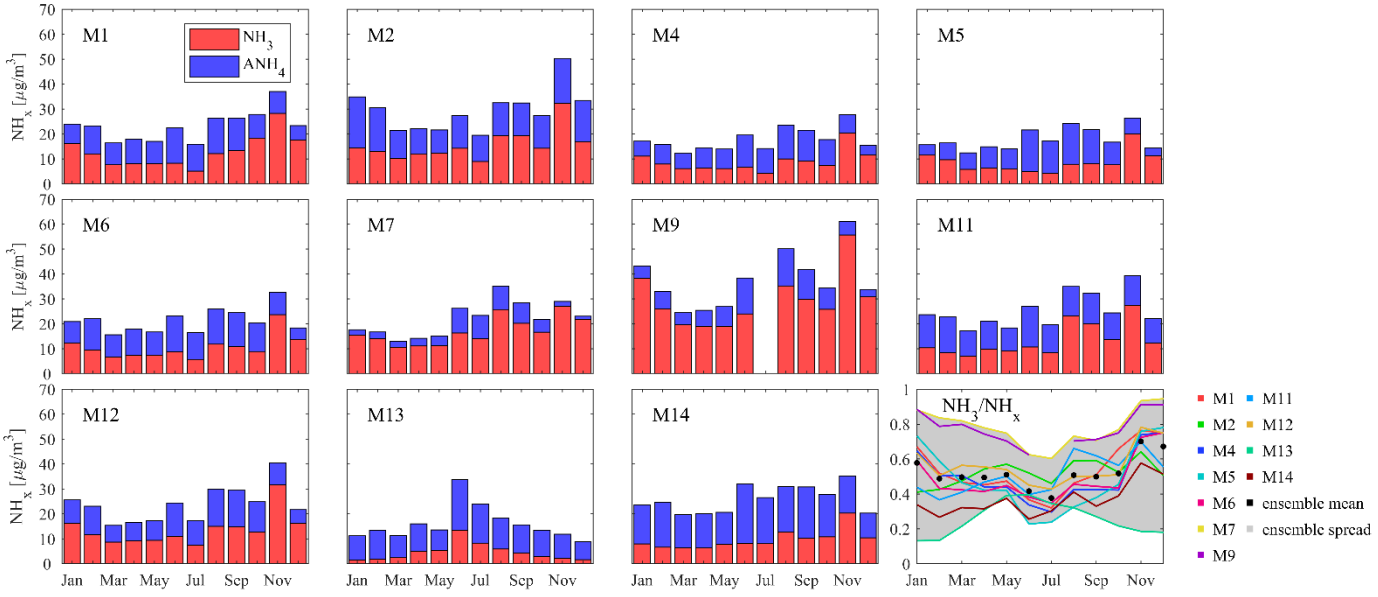

Figure 5: Timeseries of the multi-model simulated total ammonium (NH_x = NH_3 + NH_4^+) in atmosphere along with the ratio of gaseous NH_3 to the total ammonium over NCP from January to December in year 2010.

Atmos. Chem. Phys. Discuss., https://doi.org/10.5194/acp-2018-1158
Manuscript under review for journal Atmos. Chem. Phys.
Discussion started: 6 May 2019

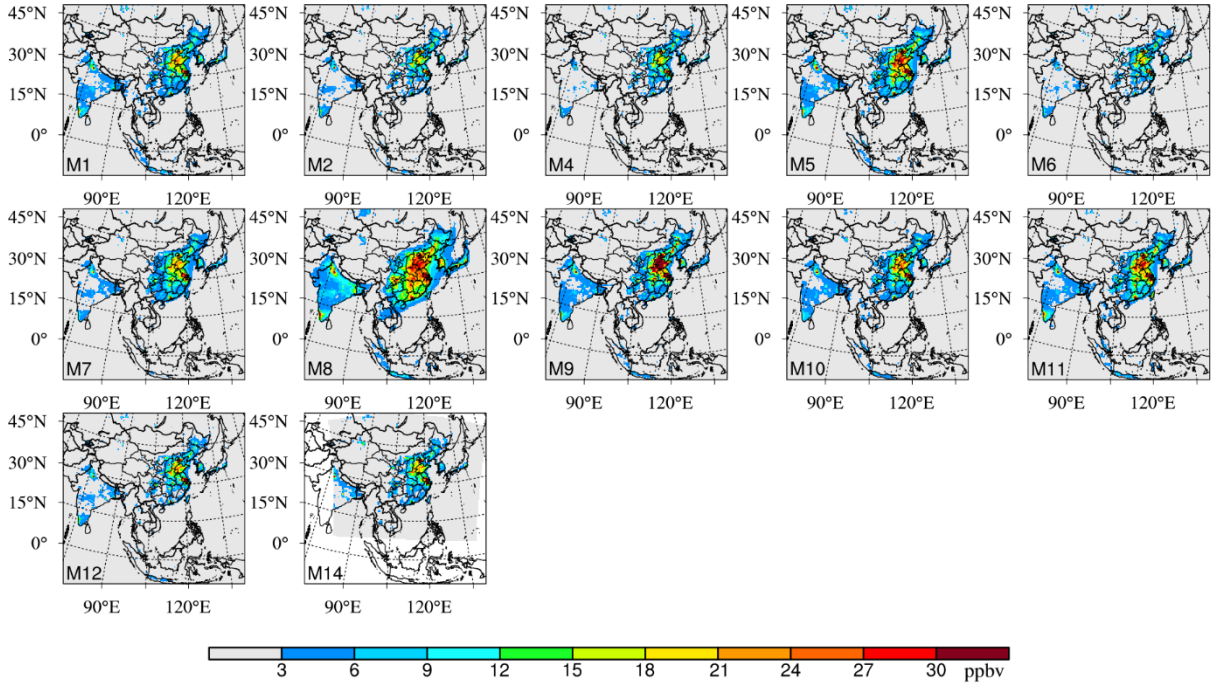

Figure 6: Spatial distribution of the annual mean NO_2 concentrations from each modeling results of MICS-Asia III. Note that M13 are not included in this figure.

Atmos. Chem. Phys. Discuss., https://doi.org/10.5194/acp-2018-1158
Manuscript under review for journal Atmos. Chem. Phys.
Discussion started: 6 May 2019

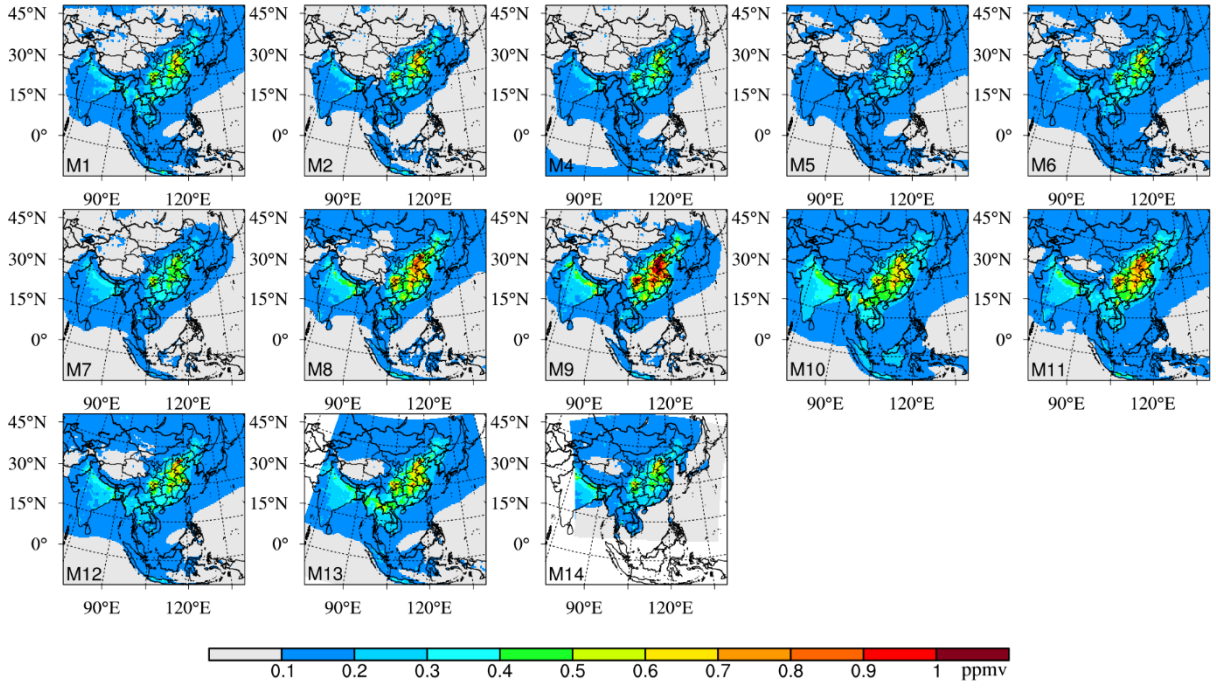

Figure 7: Spatial distribution of the annual mean CO concentrations from each modeling results of MICS-Asia III.

Atmos. Chem. Phys. Discuss., https://doi.org/10.5194/acp-2018-1158
Manuscript under review for journal Atmos. Chem. Phys.
Discussion started: 6 May 2019

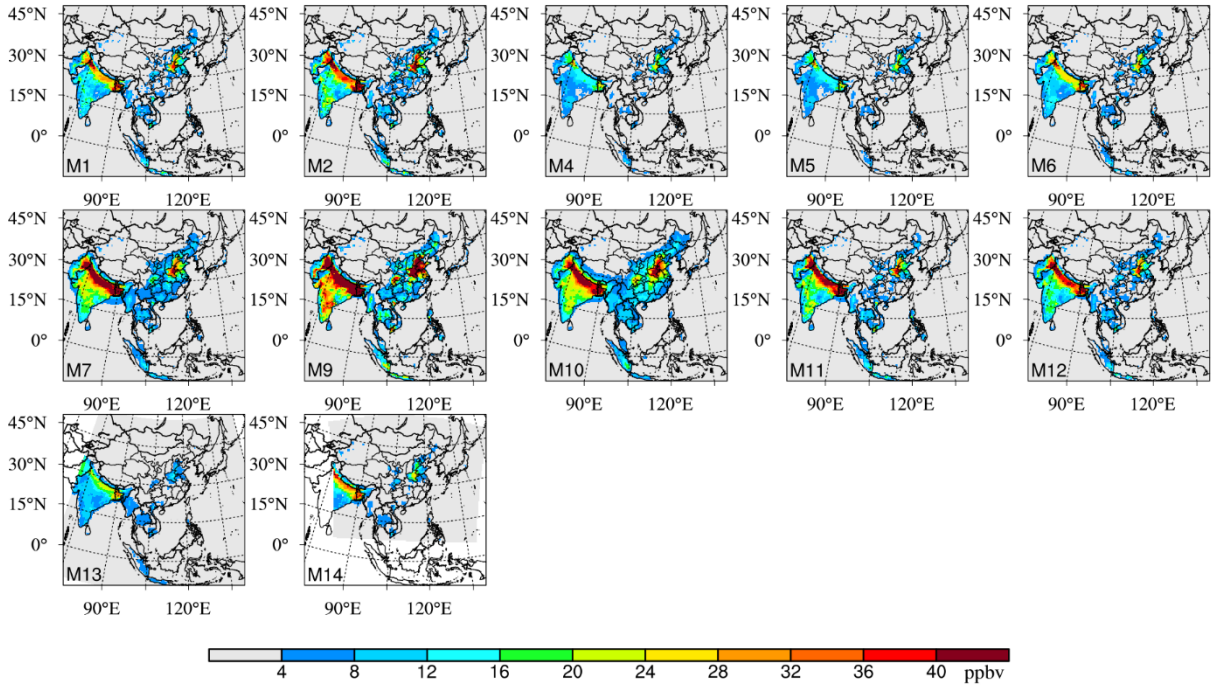

Figure 8: Spatial distribution of the annual mean NH_3 concentrations from each modeling results of MICS-Asia III.

Atmos. Chem. Phys. Discuss., https://doi.org/10.5194/acp-2018-1158
Manuscript under review for journal Atmos. Chem. Phys.
Discussion started: 6 May 2019

Atmospheric Chemistry and Physics Discussions

(a) NH_3:

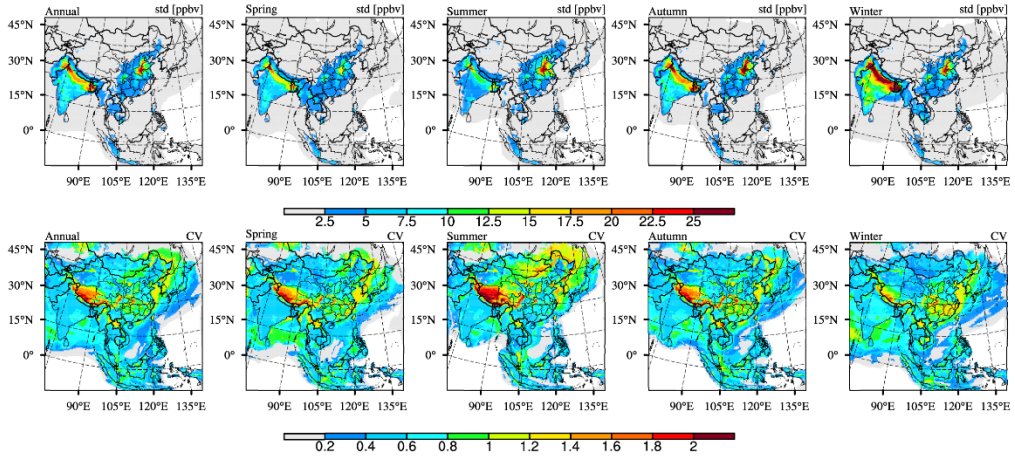

(b) CO:

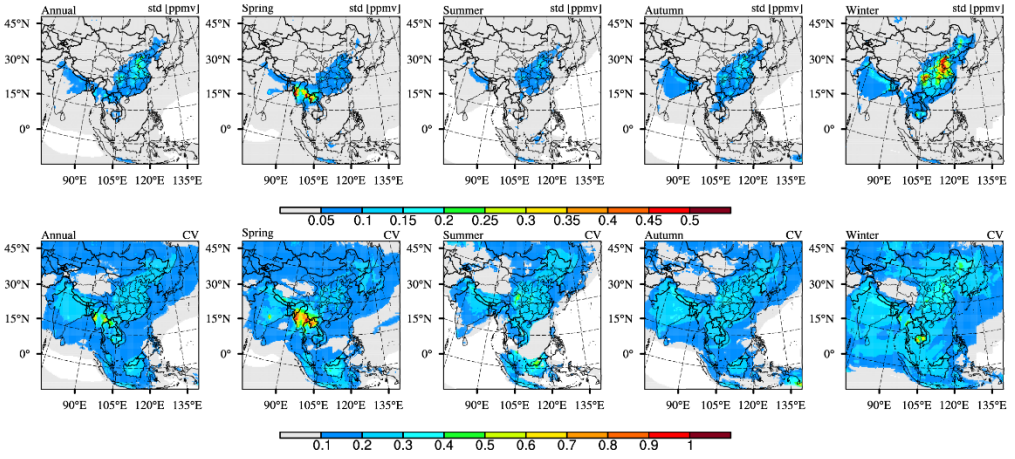

(c) NO_2:

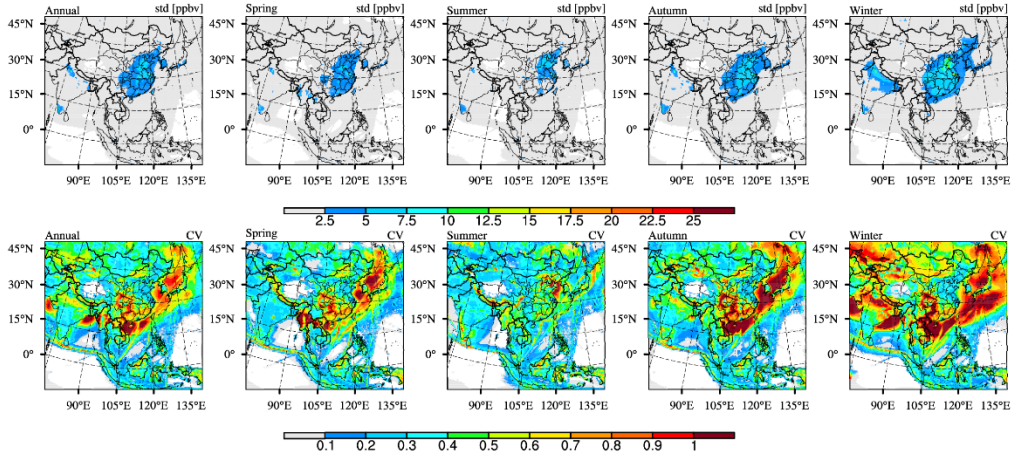

Figure 9: Spatial distribution of the standard deviation of (a) NH_3, (b) CO and (c) NO_2 multi-model predictions in MICS-Asia III, as well as the corresponding distribution of CV on the annual and seasonal basis.